



KAUNAS UNIVERSITY OF TECHNOLOGY

FACULTY OF CHEMICAL TECHNOLOGY

Ronit Sebastine Bernard

**Synthesis and properties of triphenylethylene derivatives containing
carbazole and acridine moieties**

Master's Final Degree Project

Supervisor
prof. Juozas Vidas Gražulevičius

Consultant
Galyna Sych

Kaunas, 2018



KAUNAS UNIVERSITY OF TECHNOLOGY
FACULTY OF CHEMICAL TECHNOLOGY

**Synthesis and properties of triphenylethylene derivatives
containing carbazole and acridine moieties.**

Master's Finale Degree Project, Chemical Engineering (621H81004)

Ronit Sebastine Bernard
Project author

**(HOD) prof. Juozas Vidas
Grazulevicius**
Supervisor

Dr. Jonas Keruckas
Reviewer

lekt. Valatkienė Loreta
Professor for safety and health

Kaunas, 2018

**KAUNAS UNIVERSITY OF TECHNOLOGY
FACULTY OF CHEMICAL TECHNOLOGY**

Confirmed by:
Dean of Faculty of Chemical Technology
Prof. dr. E. Valatka
Order of Dean No. ST18-F-02-3
11/04/2018

Agreed by:
Head of Department of Polymer Chemistry and
Technology
Prof. dr. J. V. Gražulevičius
/05/2018

THE TASK OF MASTER'S DEGREE FINAL PROJECT

Issued for student **Ronit Sebastine Bernard**

1. Theme of the project: **Synthesis and properties of triphenylethylene derivatives containing carbazole and acridine moieties**

2. Aim and tasks of the project.

Aim of the project Synthesis of new materials exhibiting aggregation induced emission enhancement as emitters for OLEDs.

Tasks of the project: Synthesis of compounds based on 3,6-ditertbutylcarbazole or 9,9-dimethylacridine donors. Characterization of the chemical structures of the synthesized compounds. Investigation of the photophysical properties of the obtained compounds. Investigation and interpretation of thermal, photoelectrical, and charge-transporting properties of the target compounds. Testing of the newly synthesized emitters in OLEDs.

3. Components of the final project:

- Title and headline pages;
- The task of master degree final project;
- Declaration of Academic Integrity signed by the project author;
- Abbreviations;
- Table of contents;
- Summary in Lithuanian and English languages;
- Introduction;
- Experimental:
 - Instrumentation;
 - Materials
 - Methodologies
- Results and discussion:
 - Photophysical properties
 - Aggregation Induced Emission Enhancement
 - Photoelectrical and charge-transporting properties
 - Thermal properties
 - Device fabrication and characterization
- Graphic part:
 - Principal technological scheme;
 - Drawing of the device.
- Safety and health of employee;
- Conclusions;
- References.

Assignment date of the task is 1st of March 2018.

Deadline for submission of completed work is 24th of May 2018.

Supervisor: prof. dr. Juozas Vidas Gražulevičius
(name surname)

(signature, date)

I received the task: Ronit Sebastine Bernard

(name surname of student)

(signature, date)



Kaunas University of Technology

**FACULTY OF CHEMICAL TECHNOLOGY/DEPARTMENT OF POLYMER
CHEMISTRY AND TECHNOLOGY**

Ronit Sebastine Bernard

Master's, Chemical Engineering (621H81004)

**Synthesis and properties of triphenylethylene derivatives
containing carbazole and acridine moieties**

Declaration of Academic Integrity

I confirm that the final project of mine, Ronit Sebastine Bernard, on the topic Synthesis and properties of triphenylethylene derivatives containing carbazole and acridine moieties is written completely by myself; all the provided data and research results are correct and have been obtained honestly. None of the parts of this thesis have been plagiarised from any printed, Internet-based, or otherwise recorded sources. All direct and indirect quotations from external resources are indicated in the list of references. No monetary funds (unless required by law) have been paid to anyone for any contribution to this project.

I fully and completely understand that any discovery of any manifestations/case/facts of dishonesty inevitably results in me incurring a penalty according to the procedure(s) effective at Kaunas University of Technology.

(name and surname filled in by hand)

(signature)

Table of contents

1. Introduction.....	14
2. Literature review	16
2.1. Aggregation-Caused Quenching and Aggregation Induced Emission	16
2.2. Organic Light - Emitting Devices	19
2.3. Building blocks for synthesis of target compounds.....	20
2.3.1. Carbazole and its derivatives	20
2.3.2. Acridine and its derivatives	22
2.4. Coupling reaction.....	23
2.4.1. 2.4.1. Friedel-Crafts reaction.....	23
2.5. Palladium-catalysed coupling reactions.....	24
2.5.1. Heck reaction	24
2.5.2. Buchwald-Hartwig reaction	25
2.5.3. Ullmann Coupling.....	26
3. Experimental.....	27
3.1. Instrumentation.....	27
3.2. Materials.....	28
3.3. Methodologies	29
3.3.1. Synthetic route.....	29
3.3.2. General procedure for the nucleophilic substitution reaction.....	31
3.3.3. General procedure for Heck reaction.....	32
4. Results.....	35
4.1. Photophysical properties.....	35
4.2. Aggregation Induced Emission Enhancement.....	39
4.3. Photoelectrical and hole-transporting properties.....	42
4.4. Thermal properties.....	44
4.5. Device fabrication and characterization.....	46
5. Recommendations.....	51
6. Employee's Safety and Health.....	54
6.1. Characteristics of designed materials.....	54
6.2. Occupational Risk Assessment.....	54
6.3. Safe production.....	62
6.4. Hygiene standards.....	63

6.5. Fire Safety.....	64
7. Conclusions.....	65
8. Acknowledgment.....	66
9. References	67

List of figures

Fig. 1 Molecular packing arrangements of 1,4-di[(E)-styryl]benzene (Left) and its dimethylated derivative(Right).....	15
Fig. 2 (A) ACQ (B) AIE.....	15
Fig. 3 Molecule of 1,1,2,3,4,5-hexaphenylsilole (HPS) (Left); solutions and suspensions of HPS in acetonitrile–water mixtures with different fractions of water under UV light.....	16
Fig. 4 Explanations for RIR and RIV processes.....	18
Fig. 5 Schematic representation of OLED structure.....	19
Fig. 6 Molecular structures of building blocks used in the synthesis of bipolar materials.....	20
Fig. 7 synthetic strategy for acridines.....	21
Fig. 8 Two types of Friedel-Crafts reaction.....	22
Fig. 9 Mechanism of Friedel-Crafts reaction.....	22
Fig. 10 General scheme of Heck reaction.....	23
Fig. 11. The detailed mechanism of Heck reaction.....	23
Fig. 12 General scheme of Buchwald-Hartwig reaction.....	24
Fig. 13 basic mechanism of Ullmann reaction.....	25
Fig. 14 UV-VIS absorption and fluorescence spectra of toluene, THF solution and thin films of compounds.....	34
Fig. 15. Fluorescence decay curves of thin films and THF solutions.....	36
Fig. 16 (Left) Emission spectra of compounds in the THF/water mixtures with different water content. (Right) Plots of maximum emission intensities versus water content in the THF/Water mixtures.....	39-40
Fig. 17. Electron photoemission spectra of the films of four synthesized luminogens.....	41
Fig. 18 Hole and electrons drift mobility as a function of $E^{1/2}$ for the layers of BS-9, BS-10, BS-12, BS-14.....	42
Fig. 19. Time of flight transients for holes in thin layers of compounds.....	42-43
Fig. 20 TGA curves of compounds.....	44
Fig. 21 DSC curves of BS-9, BS-10, BS-12 and BS-14.....	45
Fig. 22 Energy diagram of OLEDs.....	46
Fig. 23. Normalized electroluminescence spectra of OLEDs recorded at 8V.....	47

Fig. 24. Luminance and current density of OLEDs.....	47
Fig. 25. Current efficiency of OLEDs.....	48
Fig. 26. Power efficiency of OLEDs.....	48
Fig. 27. EQE of OLEDs.....	48
Fig. 28 S1. EL spectra of 10 OLED.....	49
Fig. 29 S2. EL spectra of 12 OLED.....	49
Fig. 30 S3. EL spectra of 14 OLED.....	49
Fig 31. Schematics for reactor design.....	51

List of tables

Table 1. Absorption and emission in solution (THF); Absorption and emission on film.....	35
Table 2. Quantum yield and Time decay.....	35
Table 3. Mobility spectra of compounds.....	41
Table 4. Thermal properties of compounds.....	44
Table 5. Electroluminescence parameters of OLEDs.....	47
Table 6. physical factors standards and lab readings.....	60
Table 7. Hygiene and determined working standards.....	62

Bernard, Ronit Sebastine. Synthesis and properties of triphenylethylene derivatives containing carbazole and acridine moieties. Master's Final Degree Project supervisor:

HOD prof. Juozas Vidas Grazulevicius; Faculty of Chemical Technology, Kaunas University of Technology.

Study field and area (study field group): Masters, Chemical Engineering, TMC-6.

Keywords: OLED, AIEE, carbazole, acridine, ionization potential, photophysical properties.

Kaunas, 2018. 70 pages.

Summary

Organic electroactive compounds gained worldwide interest in the search for alternative materials for large area, flexible, lightweight, and energy efficient optoelectronic devices. In the following work, synthesis, investigation of thermal, optical properties of four triphenylethylene based derivatives of carbazole and 9,9-dimethylacridine are presented. Photophysical properties as well as aggregation induced emission properties of target luminogens were investigated and presented in this work. It was found that all the molecules showed low fluorescence intensities in solutions but intensive emission in the solid state. Solvatochromic shifts of emission bands of the solutions of four compounds depending on the solvent polarity were observed due to the donor-acceptor molecular architecture of the compounds. Thermal properties of the compounds were estimated by differential scanning calorimetry and thermogravimetric analysis, which confirmed the thermal stability of the target molecules and high morphological stability of their glasses. The investigated compounds showed glass formation abilities and high decomposition temperatures. Organic light emitting diodes were fabricated utilizing the synthesized compounds as emitting materials. The devices based on two derivatives of acridane and one derivative of carbazole as emitting layers were fabricated. The highest brightness of 5700 cd/m² and power efficiency of 3.2 lm/W was achieved for 9,9-dimethylacridine derivative with fluorinated acceptor.

Ronitas Sebastinas, Bernardas, Trifeniletileno darinių, turinčių karbazolo ir akridino fragmentus, sintezė ir savybės. Magistro baigiamasis darbas.

Katedros vedėjas prof. Juozas Vidas Grazulevicius; Kauno technologijos universitetas, Cheminės technologijos fakultetas

Studijų kryptis ir sritis (studijų kryptių grupė): Magistras, chemijos inžinerija, TMC-6.

Reikšminiai žodžiai: OLED, AIEE, karbazolas, akridinas, jonizacijos potencialas, fotofizikinės savybės.

Kaunas, 2018. 70 p.

Santrauka

Organiniai elektroaktyvūs junginiai yra pritraukę didelį tarptautinį susidomėjimą kaip medžiagos, tinkamos didelio ploto, lankstiems, lengviems ir energiją taupantiems optoelektroniniams prietaisams. Šiame darbe pristatomi keturių trifeniletileno darinių, turinčių karbazolo ir akridido fragmentus, sintezė bei terminių ir fotofizikinių savybių tyrimų rezultatai. Nustatyta, kad susintetintiems junginiams būdingas agregacijos sukeltas emisijos suintensyvėjimas. Junginių tirpalams būdinga silpna emisija, tačiau kietoje būsenoje emisija sustiprėja. Emisija taip pat priklauso nuo tirpiklio poliškumo. Diferencinės skenuojamosios kalorimetrijos ir termogravimetrinės analizės metodais įvertinti junginių gebėjimas egzistuoti stikliškoje būsenoje bei jų terminis stabilumas. Jie geba sudaryti molekulinis stiklus ir pasižymi aukštomis terminės destrukcijos temperatūros vertėmis. Gauti junginiai ištirti kaip spinduliai organinių šviesos diodų struktūrose. Buvo pagaminti prietaisai, kuriuose du akridano ir vienas karbazolo darinys panaudoti šviesos emisijos sluoksniams. Didžiausias skaistis (5700 cd/m²) ir galios efektyvumas (3,2 lm/W) buvo pasiekti prietaise su 9,9-dimetilakridano dariniu, turinčiu fluorintą akceptorį.

Abbreviations

Short form	Full form
OLEDs	organic light-emitting diodes
OFETs	organic field-effect transistors
RIM	restriction of intramolecular motions
ACQ	aggregated-caused quenching
RIR	restriction of intramolecular rotations
AIEE	aggregated induced enhanced emission
RIV	restriction of intramolecular vibrations
THBA	10,10',11,11'-tetrahydro-5,5'-bidibenzo [a, d] annulenyliene
TADF	thermally activated delayed fluorescence
DMAC	9,9-dimethyl-9,10-dihydroacridine
HOMO	highest occupied molecular orbital
LUMO	lowest unoccupied molecular orbital
PhDMAC	9,9-dimethyl-10-phenyl-9,10-dihydroacridine
NMR	nuclear Magnetic Resonance
TMS	tetramethyl silane
UV-VIS	ultra violet-visible spectroscopy
PL	photoluminescence spectroscopy
DSC	differential scanning calorimetry
TGA	thermogravimetric analysis
Hex	hexane
DCM	dichloromethane
TLC	thin layer chromatography
UV	ultra violet
DCB	dichlorobenzene
Pd	palladium
DMF	dimethylformamide
ICT	intramolecular charge transfer
PLQY	photoluminescence quantum yield

Abs	absorption
I_p	ionization potential
EA	electron affinity
E_g^{opt}	optical band gap
TOF	time of flight
T_g	glass transition temperatures
T_m	melting points
T_d	5% weight loss
NPB	N, N'-di(1-naphthyl)-N, N'-diphenyl-(1,1'-biphenyl)-4,4'diamine
TCTA	2,2',2''-tris-(N-carbazolyl)-triphenylamine
TPBi	2,2',2''-(1,3,5-benzinetriyl)-tris(1-phenyl-1-H-benzimidazole)
EL spectra	electroluminescence spectroscopy
EQE	external quantum efficiency
RCD	residual current device
PE	grounding
AC	alternate current
DC	direct current
OSHA	occupational Safety and Health Administration
TPE	triphenylethylene

1. Introduction

Utilization of organic molecules in light emitting diodes was first reported by Tang and co-workers in the year 1987 [1]. This led to the development of variety of new organic luminophores, as well as new synthetic routes for the desired materials. Nowadays a great deal of attention of scientific community is focused on the search for materials with bipolar charge transporting properties. Good charge transporting abilities afford enhance of performances of electroluminescent devices and balances hole and electron transport in the devices. It contributes to the fabrication of stable non-doped organic light-emitting diodes (OLEDs), which means the simplicity of the manufacturing process and lower costs of production. In OLEDs, organic materials are use as solid films. Due to this issue, many scientists face the problem of emission quenching of organic compounds in the solid state due to the interactions between the molecules. A big number of organic luminophores partially or completely experience effects of fluorescence quenching. Several approaches have been developed during the last decades to reduce of conquer with undesirable emission quenching effect. The most widespread ones are the utilization of host materials for the solid “dilution” of the emitting material and the second one is the implementation of rotating or non-symmetrical groups to the molecular architecture. The researchers observed that the compounds that are non-luminous in solutions but in the solid-state the compounds began to emit. This is known as aggregation induced emission enhancement phenomenon and was developed by the group of Ben Zhong Tang in 2001 [2]. The present scientific fields have much interest in the development of the luminescent materials and improve the properties for the usage in various OLEDs. A great number of experimental measurements and theoretical calculations have been performed to understand and find an explanation for the processes which operate during the aggregation process and its influence on the photophysical properties of compounds [3]. One of the possible ways to achieve the enhanced emission in solid state is rationalized restriction of intramolecular motions (RIM), including rotation, vibration, stretching, etc [4]. Synthesis of such type of materials requires careful design of the molecular structures.

The objective of work synthesis of new materials exhibiting aggregation induced emission enhancement as emitters for OLEDs. For the achievement of this objective the following tasks had to be solved.

- Synthesis of compounds based on 3,6-ditertbutylcarbazole or 9,9-dimethylacridine donors.
- Characterization of the chemical structures of the synthesized compounds.
- Investigation of the photophysical properties of the obtained compounds.

- Investigation and interpretation of thermal, photoelectrical, and charge-transporting properties of the target compounds.
- Testing of the newly synthesized emitters in OLEDs.

In our work we present four bipolar compounds exhibiting aggregation induced emission enhancement which contain electron-donating 3,6-ditertbutylcarbazole or 9,9-dimethylacridine moieties, fluorinated or non-fluorinated styrene linking bridge and triphenylethylene as the “rotor” inducing emission in the aggregated state.

2. LITERATURE REVIEW

2.1. AGGREGATION-CAUSED QUENCHING AND AGGREGATION INDUCED EMISSION

The phenomenon of emission quenching in the solid state is named aggregation-caused quenching (ACQ) which was discovered by Förster in 1954 [5]. In this case a lot of planar or close to planar compounds are experiencing intense intermolecular π - π stacking interactions [6] (Fig-1), which result in the emission quenching of the luminophores. It might also form aggregates in the aqueous solvent due to its increased hydrophobic properties. Hence the (ACQ) is not efficient in development of optoelectronic devices like OLEDs [7].

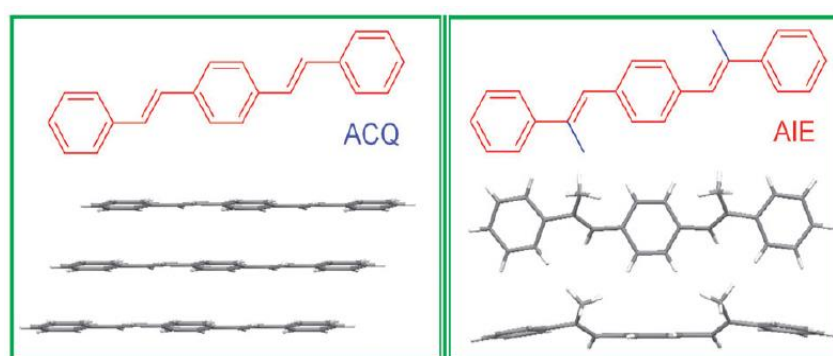


Fig. 1. Molecular packing arrangements of 1,4-di[(E)-styryl]benzene (Left) and its dimethylated derivative(Right)

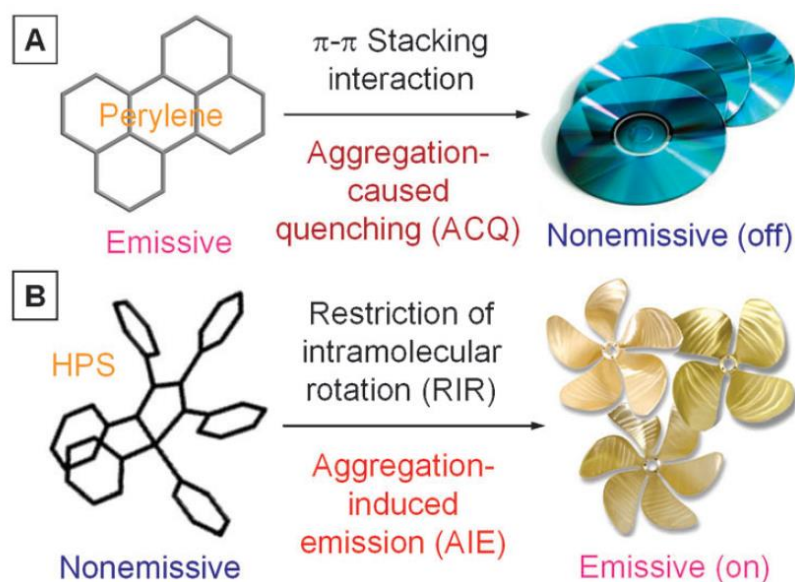


Fig. 2 (A) ACQ (B) AIE

Fig. 2. (A) Planar molecule (for example perylene) is aggregating as discs, due to the strong π - π stacking interactions between the aromatic rings, which leads to the no or low light emission. (B) Non-planar molecules such as hexaphenylsilole (HPS), consisting of six phenyl

rotating groups, are highly emissive by aggregate formation, due to the restriction of the intramolecular rotation (RIR) of the phenyl rotors against the silole stator.

To overcome or reduce the notorious ACQ effect several approaches have been developed and investigated [8]. The most widespread ones are the utilization of host materials for the solid “dilution” of the emitting material and second is the implementation of rotating or non-symmetrical groups to the molecular architecture.

In the second method researchers observed that the compounds that are non-luminous in a solvent but while aggregation the compound began to emit. This phenomenon is known as Aggregated Induced Emission (AIE) or Aggregated Induced Enhanced Emission (AIEE) (if compound has low emission in solution but highly emissive in solid state) and was firstly observed during synthesis and investigation of 1-methyl-1,2,3,4,5-pentaphenylsilole by group of Ben Zhong Tang in 2001. Due to the experimental data of 1-methyl-1,2,3,4,5-pentaphenylsilole, the quantum efficiency was changing from 0.06% in ethanol solution to 21% in solid state.

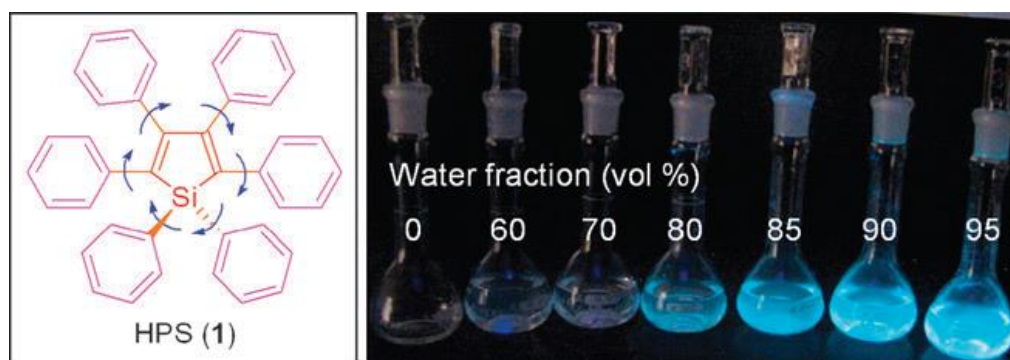


Fig. 3. Molecule of 1,1,2,3,4,5-hexaphenylsilole (HPS) (Left); solutions and suspensions of HPS in acetonitrile–water mixtures with different fractions of water under UV light;

After this the same phenomenon was observed in other “silole”- based compounds creating a big AIE family of 1-substituted -1,2,3,4,5-pentaphenylsilole (Fig-3) [9a, b]. It was observed that ‘silole’ does not luminesce when dissolved but starting so upon aggregation. This motivated and attracted attention of a lot of researches in the field of highly luminescent materials to improve the efficiency of materials in the solid state and usage in non-doped OLEDs [10].

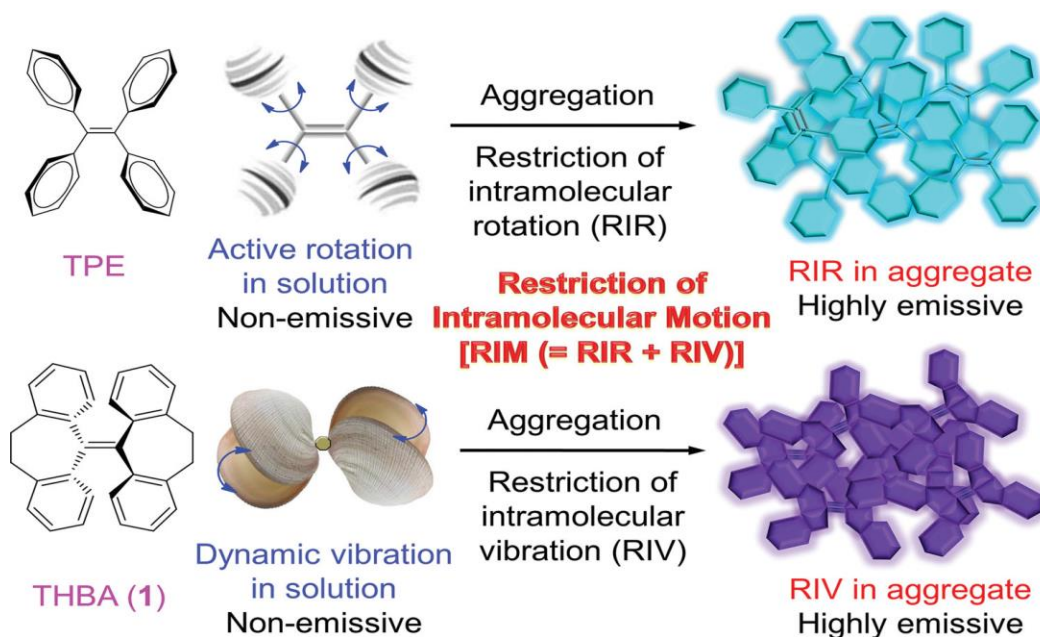


Fig. 4. Explanations for RIR and RIV processes

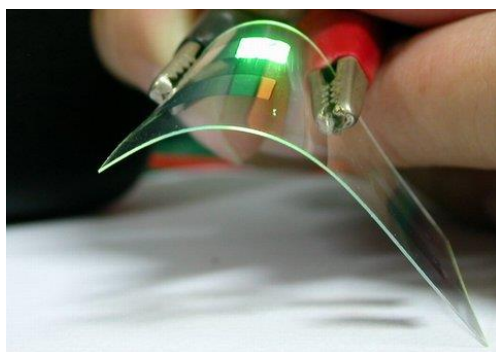
One of the reasons of AIE phenomenon is the restriction of intramolecular motions (RIM), which include such mechanisms as of restriction intramolecular rotation (RIR) and restriction of intramolecular vibrations (RIV). It was observed that RIR mechanism is responsible for the aggregation emission enhancement of molecular rotors. As it was abovementioned, AIE was observed in HPS molecule, where six phenyl rings are tethered to a silole core and are dynamically rotating against the silole stator [10]. One of the another well-studied AIEgen example is tetra-phenylethene (TPE)(Fig-4), in which four phenyl rings are connected to a central ethylene core through single bonds. Isolated molecules in dilute solution are non-emissive due to the active intramolecular rotations, which lead to the low or no emission in solution. However, while aggregation the intramolecular rotations are highly restricted because of physical constraint, which leads to the high emission in aggregate state [11]. Still a lot of molecules which are not carrying any rotating groups in their structure are possessing AIE effect. One of them is as 10,10',11,11'-tetrahydro-5,5'-bidibenzo [a, d] annulenyldiene (THBA) (Fig-4), which consist of two non-coplanar flexible parts. This flexibility allows the phenyl rings of THBA to bend or vibrate in the solution state, but upon aggregation due to the physical constraint the intramolecular vibrations become restricted. Such a restriction results in effective emission in the solid aggregate state. The quantum efficiency of solution of THBA molecule was found to be less than 0,1%, then in aggregate state – 23%, which is due to the efficient restriction of intramolecular vibrations. The leading mechanism in THBA is RIV process.

- (a) Electrostatic attraction – in this the attraction of two molecules with opposite charges is occurred.
- (b) Hydrogen bonding – here the dipole-dipole interactions is observed. The materials with hydrogen atom interacts with the halogens. The bonding is occurred at the electron negative position, where the halogen interacts with the hydrogen and forms a by-product. Thus, creating and vacancy for the hydrogen in donor group to bond with the carbon atom in the acceptor group. This type of mechanism is also called as donor-acceptor interaction.
- (c) Hydrophobic effect – here we can observe that, the formation of aggregates is due to the presence of non-polar molecules in the compound. H₂O with high polarity causes the non-polar molecules to move towards the cavities with low polarity inside the structure or compound, and with less volume in the structure the compounds tend to form the aggregates with restricted intramolecular motions [12].

The development of organic materials with low molar mass has a wide range of research spectrum. Highly emissive AIE luminogens have found a variety of technological applications such as OLEDs, biological probes, miscellaneous systems, and chemical sensors. Great interest is focused on the investigation of their utilities in the development of OLEDs and sensory systems [13].

2.2. ORGANIC LIGHT - EMITTING DEVICES

Organic light - emitting diodes (OLEDs) are receiving great attraction as a perspective type of display technology due to their high colour rendering, high flexibility, and low power consumption [14]. The emissive electroluminescent layer of organic device is a film of organic material that emits light in response to provided electric charge that transform electrical energy into light [15]. Usually OLEDs are based on two types of amorphous organic semiconductors: devices employing small molecules and those employing polymers. With the different size, the molecules contain cyclic conjugated double bonds that make the material an organic semiconductor [16].



OLED structure

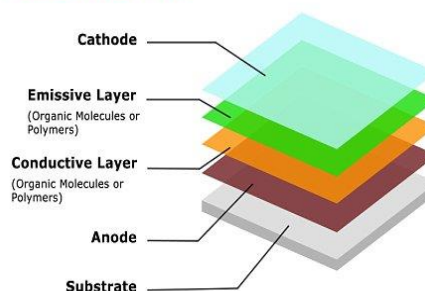


Fig. 5. Schematic representation of OLED structure

There are three main types of electroluminescence mechanisms in OLEDs: fluorescence (realizing 25% of singlets excitons), phosphorescence (realizing 75% of triplet's excitons), and thermally activated delayed fluorescence (TADF) (up to 100% of both singlets and triplets) [17].

There are three main different types of compounds used in an OLED:

- **Hole-transport materials:** Easily oxidized and conduct positive charges (holes).
- **Electron-transport materials:** Easily reduced and conduct negative charges (electrons).
- **Emissive materials:** Holes and electrons recombine and emit light.

The materials with low mass are also called as amorphous molecular materials. Researchers are developing new and effective ways for the synthesis of the organic compounds [ref-10].

The amorphous materials can be layered on the film by different ways:

- Vacuum deposition technique;
- Solution based processes (spin coating, drop casting);

2.3. BUILDING BLOCKS FOR SYNTHESIS OF TARGET COMPOUNDS

2.3.1. Carbazole and its derivatives

Stable compounds are of great interest for the implementation in highly efficient OLED's and other fields of optoelectronics [18]. For the synthesis of target AIEE luminogens we have chosen di-*tert*-butyl carbazole and 9,9-dimethyl-9,10-dihydroacridine (DMAC) as the electron-donating part of the molecules. Carbazole and 9,9-dimethyl-9,10-dihydroacridine and their derivatives (Fig-6) are one of the major building blocks which are widely used for the synthesis of bipolar compounds. These materials are effective due to their sufficiently high

triplet energy, wide band gaps, as well as efficient charge transport and excellent thermal properties.

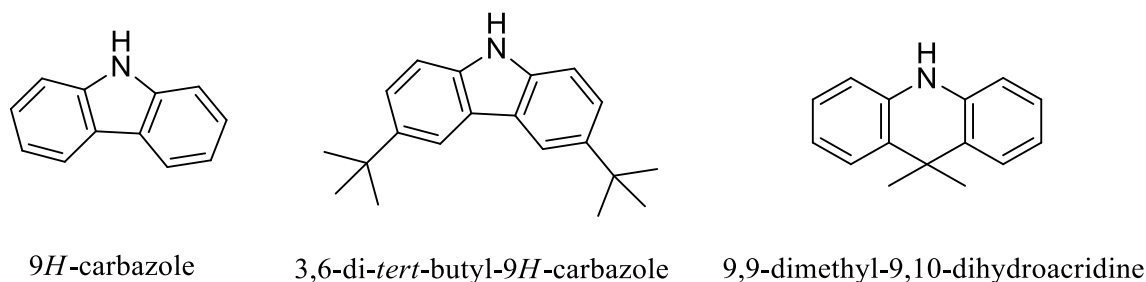


Fig. 6. Molecular structures of building blocks used in the synthesis of bipolar materials.

Carbazole moiety is possessing with excellent hole-transporting abilities and high ionization potential [19]. Carbazole has several advantages for the application in synthesis of materials for optoelectronics:

- High electrical conductivity;
- High energy of highest occupied molecular orbital (HOMO) and low energy of lowest unoccupied molecular orbital (LUMO) which lead to high band gap value;
- Balanced process of charge transporting in the device;
- Possibility of addition or introduction of new and different subunits to aromatic rings;
- Synthesis of carbazole and its derivatives is easy and at low cost.

Carbazole can be modified by substituting of different position of both phenyl rings or N-9 positions, presenting in carbazole structure, giving us the opportunity to design and investigate compounds with different and suitable properties. Carbazole based materials are used in many devices like OLED's, solar cells, and OFETs. These compounds have low molecular weight making them ideal for this type of applications in the devices [20]. Taking this into account, the molecules based on modified carbazole and 9,9-dimethyl-9,10-dihydroacridine were used for the synthesis of new AIE luminogens. In our approach, we have linked non-fluorinated and fluorinated styrene to the NH-position of electron donating moieties (both 3,6-di-*tert*-butyl carbazole and 9,9-dimethyl-9,10-dihydroacridine) by Buchwald-Hartwig reaction for non-fluorinated styrene and by using nucleophilic substitution reaction for 2,3,4,5,6-fluorinated styrene. For the activation of phenomenon of aggregation induced enhanced emission, widely used triphenyl ethylene AIE rotor was introduced in the previously synthesized molecules by Heck reaction of vinyl group and 1-bromo-1,2,3-triphenylethylene.

2.3.2. Acridine and its derivatives

Acridine was identified in 1870 by Graebe and Caro. It has attracted a lot of attention due to the interesting properties. The general applications of acridine are mainly biologically like drugs, dyes, or sensors and used for environmental chemo sensors [21]. For the last decades, the derivatives of acridine are being used as building blocks for optoelectronic application because of its conjugated structure, giving researchers a new way for the modification of molecular structures. Hence, several synthetic approaches have been developed for the synthesis of different acridine derivatives. Ring closure reaction is one of the most effective techniques used for the synthesis of acridine derivatives. The derivative can be obtained by modification of aromatic rings with suitable precursors and positions, by using ring closure reactions. In addition to this method rearrangement, oxidation, and reduction can also be used to synthesize acridine [22].

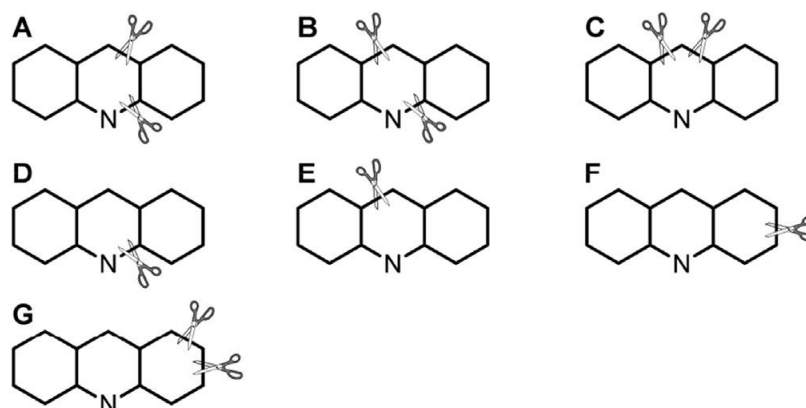


Fig. 7. synthetic strategy for acridines

One of the most widely used derivative of acridine is 9,9-dimethyl-9,10-dihydroacridine (DMAC). DMAC serves as the efficient backbone for big variety of hole-transporting materials, host materials and emitters for OLEDs [23]. The derivative can be modified in three more positions like the phenyl backbone, nitrogen atom and bridged carbon atom. Lee et al. developed a hole transporting material for OLEDs by introducing a small amount of the hole-transport moieties on the C9-position [24]. Adachi et al. used one of the acridine derivative, 9,9-dimethyl-10-phenyl-9,10-dihydroacridine (PhDMAc), to construct the emitters by using thermally activated delayed fluorescence (TADF) [25].

Advantages of acridine and its derivatives:

- High thermal stability;
- High energy of triplet states.
- Possibility of simple modification.
- Bipolar charge transfer.

Disadvantages

- Commercial product, hence slightly costly.
- Multi step combining mechanism.

2.4. COUPLING REACTION

2.4.1. Friedel-Crafts reaction

Friedel-Crafts reaction is one of the oldest organic carbon-carbon formation reaction developed by Charles Friedel and James Crafts in 1877 as the reaction of attachment of substituents to an aromatic ring. There are two main types of Friedel-Crafts reactions: alkylation reactions and acylation reactions [26]. Both types of reaction are reaction of electrophilic aromatic substitution. Friedel-Crafts alkylation is the alkylation of an aromatic ring with an alkyl halide using a strong Lewis acid such as AlCl_3 , FeCl_3 or ZnCl_2 .

On the first step of the reaction alkyl halide reacts with the Lewis acid to form electrophilic carbocation. On the second step the π -electrons of the aromatic ring act as a nucleophile, attacking the electrophilic alkyl carbocation resulting in the formation of target alkylated product Fig-8 [27].

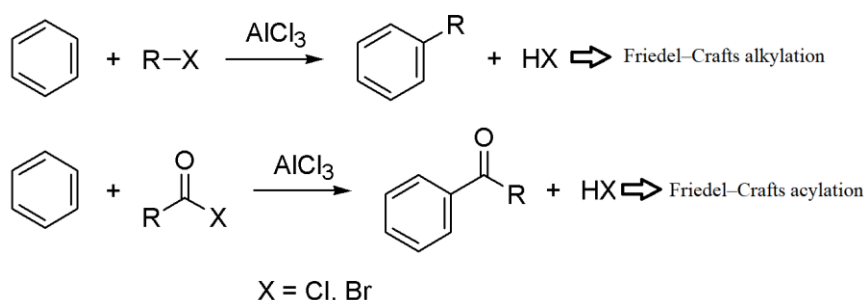


Fig. 8. Two types of Friedel-Crafts reaction.

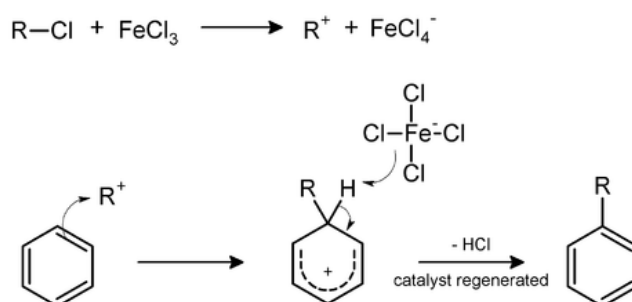


Fig. 9. Mechanism of Friedel-Crafts reaction.

2.5. Palladium-catalysed coupling reactions

2.5.1 Heck reaction

The cross-coupling reaction of an organohalides and alkene in the presence of the palladium catalyst and base is called as Heck reaction:

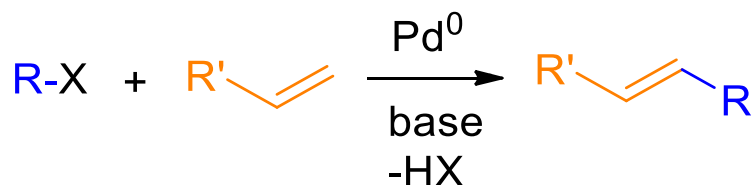


Fig. 10. General scheme of Heck reaction

It was discovered by Mizoroki and Heck in 1972 through independent research. In 2010 Richard F. Heck was awarded Nobel Prize in Chemistry for the discovery and development of his reaction. The halide ($\text{I} > \text{OTf} > \text{Br} > \text{Cl}$) is an aryl, benzyl, or vinyl compound and the alkene is electron-deficient, which contains at least one hydrogen in its structure. The most famous catalyst are tetra-kis(triphenylphosphine)palladium (0), palladium chloride or palladium(II) acetate. The ligand is triphenylphosphine or BINAP. The base is triethylamine, potassium carbonate or sodium acetate.

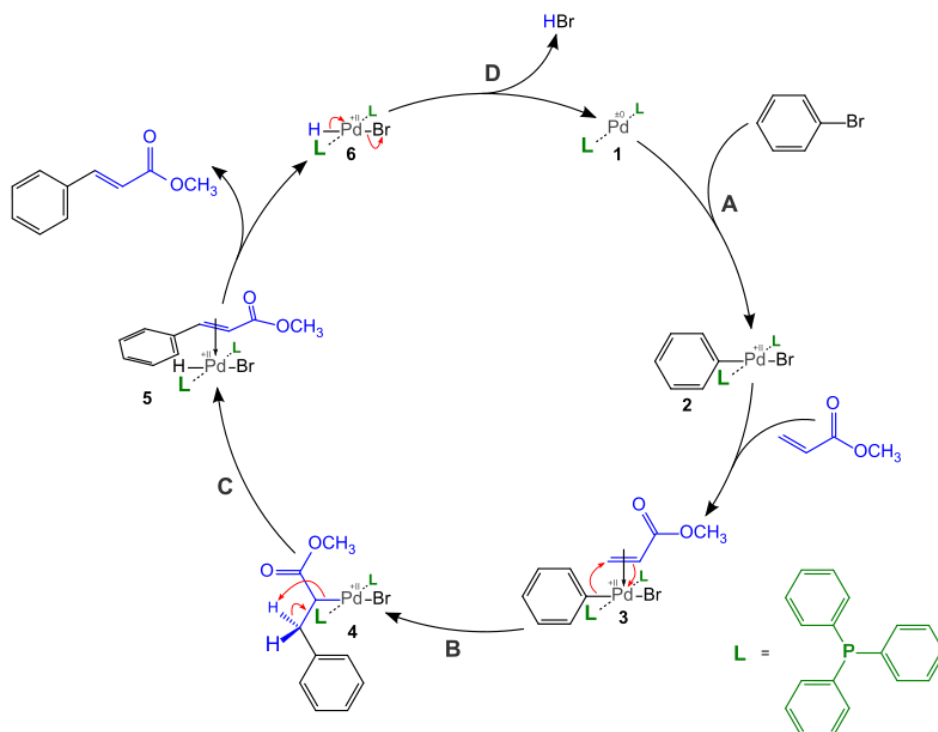


Fig. 11. The detailed mechanism of Heck reaction.

The mechanism has several steps around the palladium catalyst (Fig-11). The first step (step A) is an oxidative addition of a polar substrate onto a palladium catalyst to form a tetra-substituted π -complex. During the step B olefin is migrating and inserting into the system with the next elimination of the alkene (step C). On the last step (step D) base is connecting to the palladium to regenerate the starting catalyst and close the cycle.

2.5.2. Buchwald-Hartwig reaction

Buchwald-Hartwig reaction is the reaction for the synthesis of carbon-nitrogen bonds. Amines and aryl halides are cross coupled with palladium catalyst. The development of the mechanism was done by Stephen L. Buchwald and John F. Hartwig, who published from year 1994 to 2000's that showed a scope in this reaction.

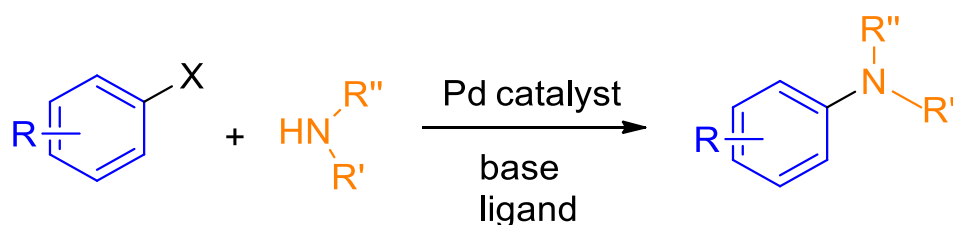


Fig. 12. General scheme of Buchwald-Hartwig reaction.

In the reaction mechanism the aryl halide was bonded with palladium (0) by oxidative addition. palladium (0) is believed to form the palladium (II) in the previous step. In the second step the co-ordination of amine is occurred with palladium through a ligand exchange. The 3rd step involves the addition of the base to the mixture. Here in 3rd step base will separate the “H” proton and the halide from the palladium chain, making vacancy for the “N” proton to bond with the palladium forming a covalent bond, this is called as substitution mechanism. In the 4th step the elimination of palladium is occurred by reductive elimination, this leads to the finale product of the reaction, the finale product is called as “Aryl-amine”. However, a side reaction can occur wherein β -hydride elimination followed by reductive elimination produces the hydro-de-halogenated arene (Aromatic hydrocarbon) and the corresponding imine (functional group with carbon-nitrogen double bond).

2.5.3. Ullmann Coupling

It is a coupling reaction between aryl halides and copper. The reaction is named after Fritz Ullmann. The traditional version of the Ullmann reaction requires harsh reaction conditions, and the reaction has a reputation for good yields. Since its discovery some improvements and alternative procedures have been introduced.

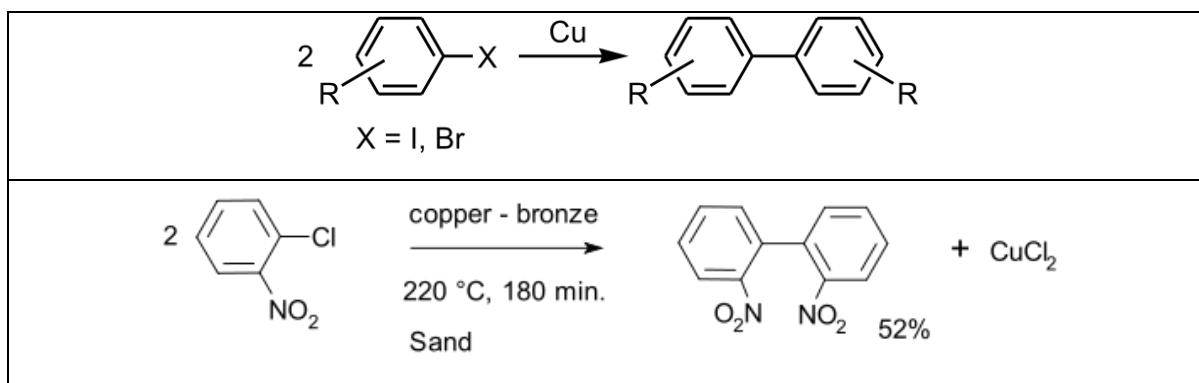


Fig. 13. basic mechanism of Ullmann reaction

It is also called as “Dimerization reaction”, here we have two aryl halides as shown in (Fig 13). The catalyst used is copper. It helps in the breaking of c-halogen bonds of the two molecules. This creates the vacancy near the carbon bonds of two halogens, and they bond together with c-c bonding by forming a σ -bond. The two halogens are stabilized using copper. The final product formed in this reaction is called a “Dimer”.

3. Experimental

3.1. Instrumentation

NMR: Nuclear Magnetic Resonance

NMR allows the observation of specific quantum mechanical magnetic properties of the atomic nucleus. NMR phenomena is used to study molecular physics, crystals, and non-crystalline materials through nuclear magnetic resonance spectroscopy. ^1H and ^{13}C nuclear magnetic resonance (NMR) spectra of the solutions in deuterated chloroform (CDCl_3) were recorded using Bruker DRX 400 P (400 MHz (^1H), 100 MHz (^{13}C)). Chemical shifts (δ) are reported in ppm referenced to tetramethyl silane (TMS).

UV-VIS

UV/Vis spectra of 10^{-4} M solutions and thin films of the compounds were recorded in quartz cells by Perkin Elmer Lambda 35 spectrometer.

Photoluminescence spectra

PL-spectra of 10^{-5} M solutions and thin films were recorded using Edinburgh Instruments' FLS980 Fluorescence Spectrometer. Thin solid films were prepared by drop casting technique from 1 mg/ml solution of compound in THF.

Differential scanning calorimetry (DSC)

DSC measurements were done with TA Instruments "DSC Q100" calorimeter. The samples were heated at a scan rate of $10\text{ }^\circ\text{C}/\text{min}$ under nitrogen atmosphere.

Thermogravimetric analysis (TGA)

TGA measurements were done with "Mettler TGA/SDTA851e/LF/1100" at a heating rate of $20\text{ }^\circ\text{C}/\text{min}$ under nitrogen atmosphere.

Photoelectron emission

Photoelectron emission spectra for vacuum deposited layers of the studied compounds were recorded to obtain the solid-state ionization potentials of the compounds.

Device measurement

Electroluminescence (EL) spectra were measured using Avenues AvaSpec-2048XL spectrometer. Fabrication of OLEDs was done by step-by-step vacuum-deposition of organic and metal layers onto precleaned patterned ITO-coated glass substrates with a sheet resistance of $150\ \Omega/\text{sq}$ under the vacuum of 2×10^{-6} mBar. Layers were deposited using vacuum equipment from Kurt J. Lesker in-built in an MB EcoVap4G glove box with the deposition rate of $\sim 1\text{-}2\ \text{\AA}/\text{s}$ for organic materials. Density-voltage and luminance-voltage records were made simultaneously by using calibrated PH100-Si-HA-D0 photodiode, Keithley 6517B

electrometer, Keithley 2400C source meter and a PC-Based Power and Energy Monitor 11S-LINK. All electroluminescent investigation was done in the air at room temperature without passivation [28].

3.2. Materials

Compounds	Chemical formula	Producer
Carbazole	C ₁₂ H ₉ N	Sigma-Aldrich
Zinc chloride	ZnCl ₂	Alfa Aesar
<i>tert</i> -Butyl chloride	C ₄ H ₉ Cl	Sigma-Aldrich
<i>tert</i> -Butyl carbazole	C ₂₀ H ₂₅ N	Synthesised in lab
9,9-dimethyl-9,10-dihydroacridine	C ₁₅ H ₁₄ N	Sigma-Aldrich
Nitromethane	CH ₃ NO ₂	Sigma-Aldrich
Sodium sulfate	Na ₂ SO ₄	Sigma-Aldrich
Silica Gel	SiO ₂	Sigma-Aldrich
Ethyl Acetate	C ₄ H ₈ O ₂	Sigma-Aldrich
Acetone	C ₃ H ₆ O	Sigma-Aldrich
Isopropanol	C ₃ H ₈ O	Sigma-Aldrich
3,6-di- <i>tert</i> -butyl-9-(2,3,5,6-tetrafluoro-4-vinylphenyl)-9Hcarbazole	C ₂₈ H ₂₇ F ₄ N	Synthesised in lab
1-Bromo-1,2,2-triphenylethylene	(C ₆ H ₅) ₂ C(C ₆ H ₅) Br	Sigma-Aldrich
Palladium (II) acetate	C ₄ H ₆ O ₄ Pd	Sigma-Aldrich
Triethyl Amine	C ₆ H ₁₅ N	Sigma-Aldrich
Dimethylformamide	C ₃ H ₇ NO	Sigma-Aldrich
Tri(<i>o</i> -tolyl) phosphene	(CH ₃ C ₆ H ₄) ₃ P	Sigma-Aldrich
10-(2,3,5,6-tetrafluoro-4-vinylphenyl)-9,10-dihydro-9,9-dimethylacridine	C ₂₃ H ₁₇ F ₄ N	Synthesised in lab
Copper	Cu	Sigma-Aldrich
Potassium carbonate	K ₂ CO ₃	Sigma-Aldrich
Tri- <i>tert</i> -butyl phosphene	[(CH ₃) ₃ C] ₃ P	Sigma-Aldrich
Potassium <i>tert</i> -butoxide	(CH ₃) ₃ COK	Sigma-Aldrich
Toluene	C ₆ H ₅ CH ₃	Sigma-Aldrich
3,6-di- <i>tert</i> -butyl-9-(4-vinylphenyl)-9Hcarbazole	C ₂₈ H ₃₁ N	Synthesised in lab
9,10-dihydro-9,9-dimethyl-10-(4-vinylphenyl) acridine	C ₂₃ H ₂₁ N	Synthesised in lab
4-Bromostyrene	CH ₂ CHC ₆ H ₄ Br	Sigma-Aldrich
Chloroform-d	CDCl ₃	Sigma-Aldrich

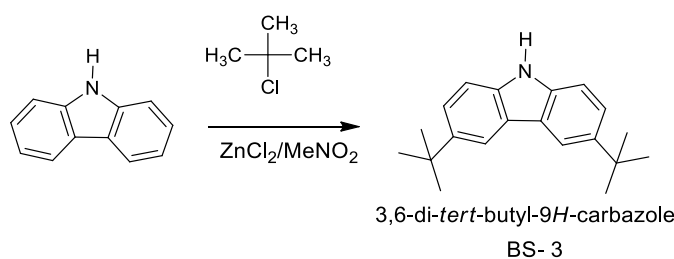
3.3. Methodologies

3.3.1. Synthetic route

All four target compounds BS-9, BS-10, BS-12 and BS-11 were synthesized by coupling reaction of previously synthesized vinyl-containing aryl part and 1-bromo-1,2,2-triphenylethylene according to the mechanism of Heck reaction (ref-38). Intermediate vinyl-containing aryls were synthesized by nucleophilic substitution reaction of Fluorine atom in pentafluoro styrene or Buchwald-Hartwig reaction of 4-bromostyrene and electron-donating di-*tert*-butyl carbazole/ 9,9-dimethylacridine.

3,6-di-*tert*-butyl-carbazole (BS-3) was obtained by the similar procedure described in literature (ref-26) and according to the mechanism of Friedel-Crafts alkylation described above (Section 2.4.1).

9H-carbazole (0.2g, 11.976 mmol) was dispersed in nitromethane (60ml), and zinc chloride (4.88g, 35.78 mmol) and 2-chloro-2-methylpropane (3.32g, 35.86 mmol) were added at 0°C. The reaction was kept overnight at room temperature. The mixture was poured in ice water, extracted with DCM, and dried with Na₂SO₄. After evaporation of the solvent, crude product was recrystallized from Hexane to obtain white crystals with yield of 95% (Scheme 1). ¹H NMR (400 MHz, CDCl₃) δ 8.10 (d, *J* = 1.7 Hz, 2H), 7.80 (s, 1H), 7.48 (dd, *J* = 8.5, 1.9 Hz, 2H), 7.33 (d, *J* = 8.5 Hz, 2H), 1.47 (s, 18H). ¹³C NMR (101 MHz, CDCl₃) δ 142.25, 138.05, 123.55, 123.34, 116.20, 110.03, 34.72, 32.07.

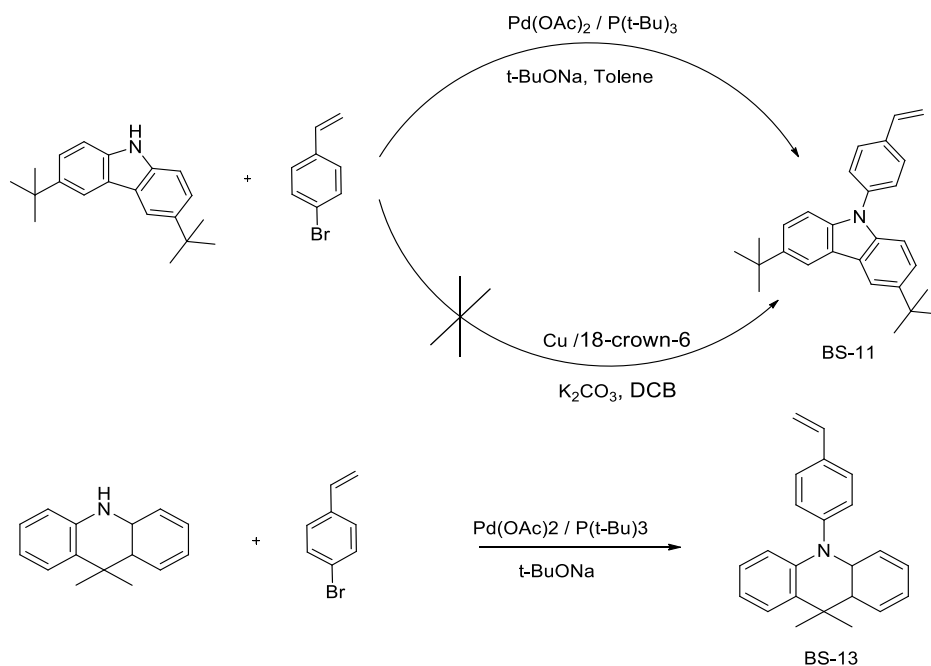


Scheme 1. Synthetic scheme of starting building block

For the synthesis of intermediate styrene-based compounds BS-11 and BS-13 several approaches were used. Our first try was the utilization of Ullmann coupling reaction between 4-bromo styrene and di-*tert*-butyl-carbazole/ 9,9-dimethylacridine due to cheaper and simple reaction procedure. During the reaction at high temperature no product could be observed on the TLC plate under UV light. We changed our synthesis strategy by using Pd-catalysed Buchwald-Hartwig reaction, which afford our products in a good yield.

3,6-di-*tert*-butyl-9-(4-vinylphenyl)-9H-carbazole (BS-11)

A mixture of di-*tert*-butyl carbazole (1g, 3.57 mmol), potassium *tert*-butoxide (1.34g, 11.94 mmol) palladium (II) acetate (0.087g, 0.387 mmol) 4-bromo-styrene (0.3ml, 2.2 mmol), tri(*tert*-butyl) phosphine (0.2ml, 0.9 mmol) in dry toluene (25 ml) under nitrogen was heated with stirring at 100 °C for 12h. After cooling to room temperature, mixture was extracted with ethyl acetate and water and dried with Na₂SO₄. Crude product was purified by column chromatography using Hex: DCM as and eluent with next recrystallization from isopropanol to afford yellowish crystals in 26 % of yield. ¹H NMR (400 MHz, CDCl₃) δ 8.19 (d, *J* = 1.3 Hz, 2H), 7.48 (dd, *J* = 8.3, 3.6 Hz, 1H), 7.39 (dd, *J* = 13.0, 8.4 Hz, 1H), 7.29 (dd, *J* = 8.6, 1.6 Hz, 2H), 7.06 (d, *J* = 7.8 Hz, 1H), 6.73 (d, *J* = 8.6 Hz, 2H), 5.78 (d, *J* = 17.6 Hz, 1H), 5.27 (d, *J* = 10.9 Hz, 1H), 1.54 (s, 1H), 1.44 (s, 18H). ¹³C NMR (101 MHz, CDCl₃) δ 143.90, 138.46, 131.81, 129.02, 127.98, 127.32, 126.75, 126.62, 124.06, 121.82, 116.49, 108.59, 34.80, 32.01



Scheme 2. Synthetic strategies for intermediate non-fluorinated compounds

8a,9,10,10a-tetrahydro-9,9-dimethyl-10-(4-vinylphenyl) acridine (BS-13)

9,10-Dihydro-9,9-dimethylacridine (0.4g, 1.911 mmol), potassium *tert*-butoxide (1.062g, 5.24 mmol) palladium (II) acetate (0.025g, 0.111 mmol), 4-bromo-styrene (0.272ml, 2.1 mmol) were charged in Schlenk flask, degassed using vacuum and filled with inert atmosphere. After 8-10 min toluene (20-25ml) was added and the mixture was stirred overnight at 100°C. After cooling to room temperature, the mixture poured in Bromo-styrene (0.272ml) flask containing

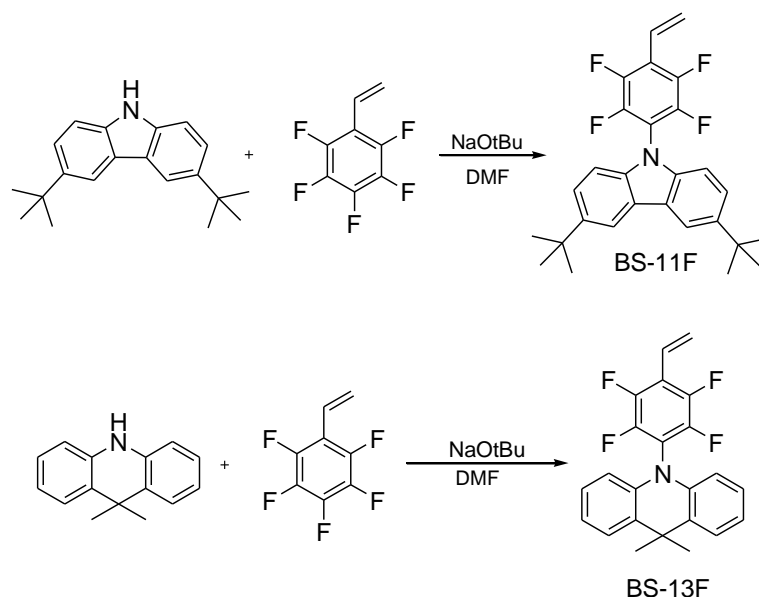
H₂O and ethyl acetate for the extraction. The organic phase was collected and dried with Na₂SO₄. The filtrate was concentrated under vacuum and purified by column chromatography. Compound was collected and recrystallized using isopropanol to afford 74 % of white solid (Scheme 2). ¹H NMR (400 MHz, CDCl₃) δ 7.67 (d, *J* = 8.3 Hz, 2H), 7.46 (dd, *J* = 7.5, 1.5 Hz, 2H), 7.30 (d, *J* = 8.3 Hz, 2H), 7.00 – 6.91 (m, 4H), 6.84 (dd, *J* = 17.6, 10.9 Hz, 1H), 6.31 (dd, *J* = 8.0, 0.9 Hz, 2H), 5.87 (d, *J* = 17.6 Hz, 1H), 5.38 (d, *J* = 10.9 Hz, 1H), 1.70 (s, 6H). ¹³C NMR (101 MHz, CDCl₃) δ 140.87, 140.66, 137.48, 136.09, 131.43, 130.00, 128.60, 126.37, 125.24, 120.55, 114.99, 114.04, 35.98, 31.29.

3.3.2. General procedure for the nucleophilic substitution reaction

General procedure for the nucleophilic substitution reaction: The mixture containing required heterocyclic compound (1 eq), sodium tert-butoxide (1.1 eq) in DMF was added dropwise to a solution of 2,3,4,5,6-pentafluoroatyrene (1.2 eq) in DMF under stirring. Reaction stirred for 10 h at room temperature, and when the solution was poured into water and extracted with EtOAc. The organic phase was dried over Na₂SO₄, filtered, and solvent was removed under reduced pressure. The crude product was chromatographed on silica gel using 5: 1 hexane–dichloromethane as an eluent (Scheme 3).

3,6-di-tert-butyl-9-(2, 3, 5, 6-tetrafluoro-4-vinyl-phenyl)-9H-carbazole (BS-11F) was prepared from 3,6-di-tert-butylcarbazole (0.3 g, 1.08 mmol), 2,3,4,5,6-pentafluoroatyrene (0.25 g, 1.3 mmol) sodium tert-butoxide (0.11 g, 1.18 mmol) and dry DMF (5 mL) according to the general procedure to give white crystals (54%). ¹H NMR (400 MHz, CDCl₃): δ 8.14 (d, *J* = 1.8 Hz, 2H), 7.50 (dd, *J* = 8.6, 1.9 Hz, 2H), 7.09 (d, *J* = 8.6 Hz, 2H), 6.82 (dd, *J* = 18.0, 11.9 Hz, 1H), 6.26 (d, *J* = 18.0 Hz, 1H), 5.84 (d, *J* = 11.9 Hz, 1H), 1.47 (s, 18H). ¹³C NMR (101 MHz, CDCl₃): δ 144.04, 138.35, 124.41, 124.04, 124.02, 122.15, 116.52, 109.31, 34.79, 31.96.

9,9-dimethyl-10-(2, 3, 5, 6-tetrafluoro-4-vinyl-phenyl)-9, 10-dihydro-acridine (BS-13F) was prepared from 9,9-Dimethyl-9,10-dihydroacridine (0.25 g, 1.2 mmol), 2,3,4,5,6-pentafluoroatyrene (0.28 g, 1.44 mmol) sodium tert-butoxide (0.13 g, 1.32 mmol) using the general procedure, and was isolated in 47% yield as a white crystal. ¹H NMR (400 MHz, CDCl₃): δ 7.42 (dd, *J* = 7.6, 1.6 Hz, 2H, Ar), 7.05 – 6.91 (m, 4H, Ar), 6.74 (dd, *J* = 18.0, 11.9 Hz, 1H, CH), 6.28 (dd, *J* = 7.9, 1.4 Hz, 2H, Ar), 6.18 (d, *J* = 18.0 Hz, 1H, CH), 5.77 (d, *J* = 11.9 Hz, 1H, CH), 1.61 (s, 6H, CH₃). ¹³C NMR (101 MHz, CDCl₃): δ 138.72, 131.31, 126.91, 125.48, 124.75, 122.15, 112.96, 36.14, 30.57.



Scheme 3. Synthetic strategies for intermediate fluorinated compounds

3.3.3. General procedure for Heck reaction

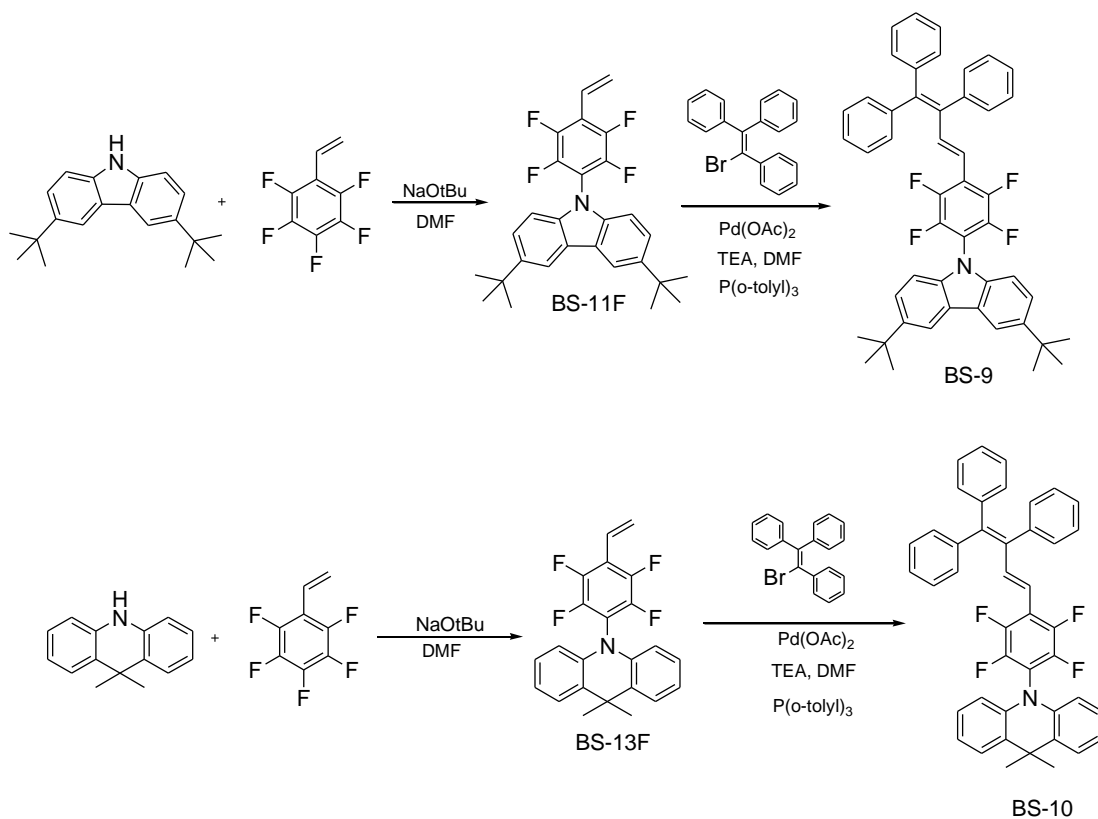
General procedure for Heck reaction: Schlenk flask was charged with 1 eq of previously synthesised intermediate compound (BS-8, BS-10a, BS-11, BS-13), 1.5 eq of 1-Bromo-1,2,2-triphenylethylene, 0.01 eq of palladium (II) acetate, 0.045 eq of tri(*o*-tolyl) phosphine, degassed and filled with inert atmosphere. Reaction was kept overnight at 140 °C. After the end of reaction (monitored by TLC) the mixture was poured into cold water and extracted with ethylacetate. The mixture was concentrated under the vacuum and crude product was purified by column chromatography with Hex:DCM (5:1) as eluent and recrystallized from isopropanol to afford a target molecule [28].

3,6-di-tert-butyl-9-(2,3,5,6-tetrafluoro-4-((E)-3,4,4-triphenylbuta-1,3-dienyl) phenyl)-9H-carbazole (BS-9):

BS-9 was prepared from BS-11F (0.2g, 0.441mmol), 1-Bromo-1,2,2-triphenylethylene (0.22g, 0.656 mmol), palladium (II) acetate (0.001g, 0.0044 mmol), tri(*o*-tolyl) phosphine (0.006g, 0.0197 mmol), triethyl amine (1.2ml) and DMF (12ml) using the general procedure and obtained as white powder in 50 % of yield. ¹H NMR (400 MHz, CDCl₃) δ 8.03 (d, *J* = 1.5 Hz, 2H), 7.59 (d, *J* = 16.4 Hz, 1H), 7.39 (dd, *J* = 8.6, 1.7 Hz, 2H), 7.37 – 7.06 (m, 11H), 7.02 – 6.93 (m, 4H), 6.87 (dd, *J* = 6.5, 3.0 Hz, 2H), 6.27 (d, *J* = 16.4 Hz, 1H), 1.40 (d, *J* = 19.0 Hz, 18H). ¹³C NMR (101 MHz, CDCl₃) δ 143.94, 131.45, 131.12, 131.06, 128.22, 128.11, 127.45, 123.97, 116.48, 109.31, 34.78, 31.97, 25.38. (Scheme 3)

10-(2,3,5,6-tetrafluoro-4-((E)-3,4,4-triphenylbuta-1,3-dienyl) phenyl)-9,10-dihydro-9,9-dimethylacridine (BS-10)

BS-10 was prepared from BS-13F (0.2g, 0.0596 mmol), 1-Bromo-1,2,2-triphenylethylene (0.262g, 0.781 mmol), palladium (II) acetate (0.00116g, 0.071 mmol), tri(*o*-tolyl) phosphine (0.07g, 0.229 mmol) triethyl amine (1.2 ml) and DMF (4 ml) using the general procedure and obtained as yellowish crystals in 55 % of yield. ¹H NMR (400 MHz, CDCl₃) δ 7.60 (d, *J* = 16.4 Hz, 1H), 7.40 (dd, *J* = 7.5, 1.6 Hz, 2H), 7.37 – 7.13 (m, 11H), 7.00 – 6.91 (m, 7H), 6.88 – 6.85 (m, 2H), 6.28 (s, 1H), 6.25 (d, *J* = 5.2 Hz, 2H), 1.59 (s, 6H). ¹³C NMR (101 MHz, CDCl₃) δ 146.78, 142.28, 141.75, 140.56, 139.24, 138.77, 131.42, 131.21, 131.11, 131.05, 128.22, 128.11, 128.03, 127.45, 127.18, 126.84, 125.38, 122.03, 118.71 – 118.54, 117.14, 112.94, 36.09, 30.49. (Scheme 4)

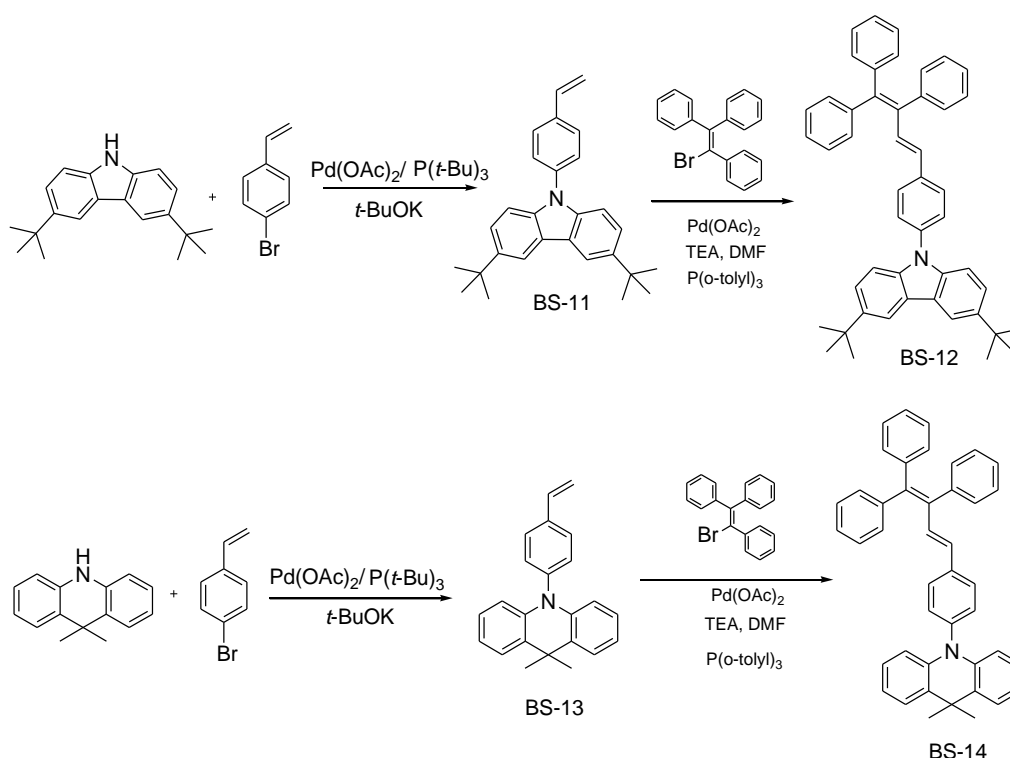


Scheme 4. Synthetic route for Fluorine-containing BS-9 and BS-10;

3,6-di-tert-butyl-9-(4-((E)-3,4,4-triphenylbuta-1,3-dienyl) phenyl)-9H-carbazole (BS-12)

BS-12 was prepared from BS-11 (0.5g, 1.31 mmol), 1-Bromo-1,2,2-triphenylethylene (0.655g, 1.953 mmol), palladium (II) acetate (0.00029g, 0.00129 mmol), tri(*o*-tolyl) phosphine (0.0175g, 0.0574 mmol), triethyl amine (3ml) and DMF (10ml) using general procedure and

obtained as yellowish crystals 42 % of yield. ^1H NMR (400 MHz, CDCl_3) δ 8.04 (d, $J = 1.6$ Hz, 2H), 7.38 – 7.32 (m, 7H), 7.29 (dd, $J = 6.9, 4.4$ Hz, 3H), 7.24 (s, 1H), 7.18 (q, $J = 6.5$ Hz, 5H), 6.99 – 6.95 (m, 3H), 6.86 (dd, $J = 6.6, 3.0$ Hz, 2H), 6.28 (d, $J = 16.0$ Hz, 1H), 1.46 (s, 2H), 1.38 (s, 18H). ^{13}C NMR (101 MHz, CDCl_3) δ 142.85, 139.09, 131.73, 131.52, 131.31, 131.14, 128.03, 127.67, 127.51, 127.38, 126.80, 126.63, 126.35, 123.58, 123.38, 116.21, 109.25, 34.74, 32.02.



Scheme 5. Synthetic route for non-fluorinated BS-12 and BS-14;

(9,10-dihydro-10-(4-((E)-3,4,4-triphenylbuta-1,3-dienyl) phenyl) acridine): DHTPBDEP-acridine(BS-14)

BS-14 was prepared from BS-13 (0.44g, 1.41 mmol), 1-Bromo-1,2,2-triphenylethylene (1.61g, 4.8 mmol), palladium (II) acetate (0.0072g, 0.032 mmol), tri(o-tolyl) phosphine (0.043g, 0.141 mmol) triethyl amine (2.64ml) and dimethyl formamide (8.8ml) using the general procedure and obtained as of yellow crystals 43 % of yield. ^1H NMR (400 MHz, CDCl_3) δ 7.35 (dd, $J = 11.7, 5.5$ Hz, 6H), 7.27 (dd, $J = 10.3, 6.2$ Hz, 4H), 7.22 – 7.14 (m, 6H), 7.12 (t, $J = 6.9$ Hz, 2H), 7.00 – 6.94 (m, 3H), 6.90 – 6.79 (m, 6H), 6.28 (d, $J = 16.0$ Hz, 1H), 6.20 (dd, $J = 7.9, 1.1$ Hz, 2H), 1.59 (s, 6H). ^{13}C NMR (101 MHz, CDCl_3) δ 142.77, 140.87, 140.07, 138.85, 132.21, 131.61, 131.50, 131.39, 131.28, 131.12, 129.99, 128.74, 128.07, 128.01, 127.55, 127.38, 126.82, 126.36, 125.18, 120.51, 114.03, 35.95, 31.22.

4. Results

4.1. Photophysical properties

To fully understand processes which are operating in our molecules, photophysical measurements, such as absorption and steady-state fluorescence spectra were performed. To understand the origin of emission, fluorescence decay curves of the compounds were recorded, and the fluorescence lifetimes were evaluated. To estimate the efficiency of emission, photoluminescence quantum yields were measured from both solution (THF) and solid state of mater (Fig. 14). Photophysical properties of all four compounds are summarized in Table 1 and Table 2. Target compounds are soluble in common organic solvents. Synthesized compounds are emitting light in blue-greenish region of the spectra in the solid state due to the similar conformational packing in the solid state.

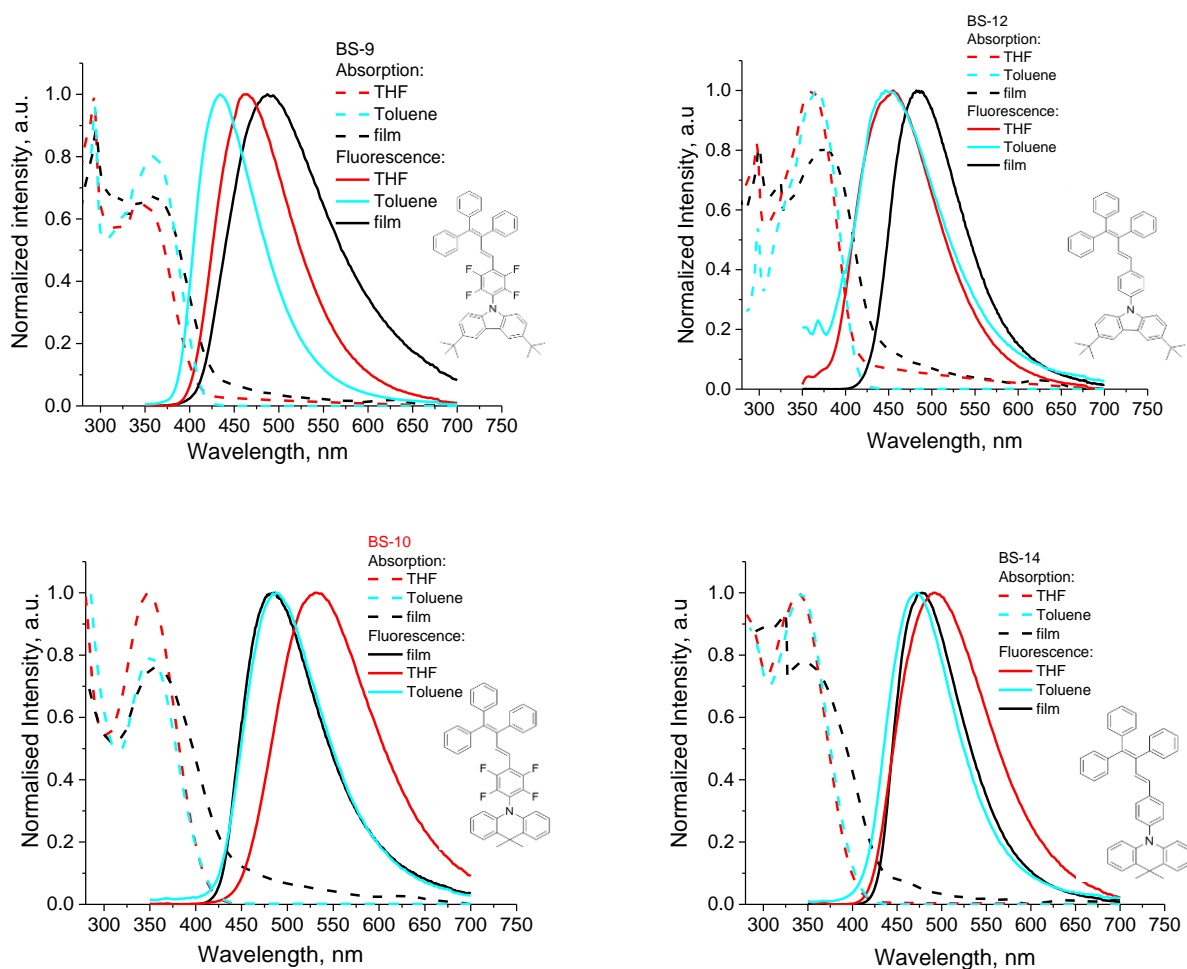


Fig. 14. UV-VIS absorption and fluorescence spectra of toluene, THF solution and thin films of compounds.

Combination of electron-donating di-*tert*-butyl carbazole or 9,9-dimethylacridine (Donors) and electron-accepting tetra-fluorobenzene offers the possibility of receiving

intramolecular charge transfer (ICT) process in molecules. To examine the dependence of molecular structure and occurrence of ICT, absorption, and emission spectrum of all four compounds were recorded in polar THF solvent and much less polar Toluene, as photophysics of the molecules containing D–A systems are strongly dependent on the solvent polarity. Obviously, the strongest ICT character was observed for compound BS-10, which consists of both stronger donor–9,9-dimethylacridine, and strong electron-accepting tetra-fluorobenzene.

Compound	$\lambda_{\text{abs}}^{\text{THF}}$ (nm)	$\lambda_{\text{abs}}^{\text{film}}$ (nm)	$\lambda_{\text{abs}}^{\text{Tol}}$ (nm)	$\lambda_{\text{em}}^{\text{THF}}$ (nm)	$\lambda_{\text{em}}^{\text{film}}$ (nm)	$\lambda_{\text{em}}^{\text{Tol}}$ (nm)	Stock shift, THF	Stock shift, film	Stock shift, Toluene
BS-9CF	348	362	357	462	487	434	114	125	77
BS-10ACF	347	360	350	532	486	485	185	126	135
BS-12C	361	377	360	455	484	448	94	107	88
BS-14AC	339	347	338	492	478	471	153	140	133

Table 1. Photophysical characteristics of compounds

$\lambda_{\text{abs}}^{\text{THF}}$ – maxima peak of last absorption band of THF solutions; $\lambda_{\text{abs}}^{\text{film}}$ – maxima peak of last absorption band of thin film; $\lambda_{\text{em}}^{\text{THF}}$ – maxima of fluorescence spectra of THF solution; $\lambda_{\text{em}}^{\text{film}}$ – maxima of fluorescence spectra of thin film; $\lambda_{\text{em}}^{\text{Tol}}$ – maxima of fluorescence spectra of toluene solution;

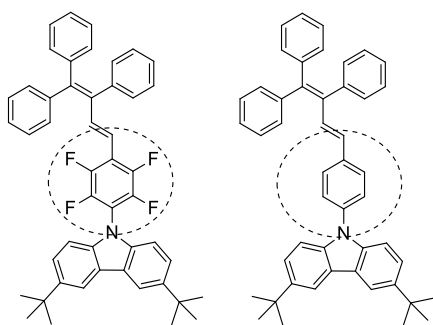
Compound	PLQY ^{THF} %	PLQY ^{film} %	τ_1/τ_2 (χ^2) ^{film} ns	τ_1 (χ^2) ^{THF} ns
BS-9CF	11	16	0.85/2.79 (1.002)	3.95 (1.004)
BS-10ACF	1	18	2.6/11.2 (1.086)	1.62 (1.094)
BS-12C	0.1	17	1.57/- (1.054)	0.33 (1.095)
BS-14AC	2	29	1.45/5.39 (1.010)	0.85 (1.011)

Table 2. Quantum yield and fluorescence lifetimes

PLQY^{THF} – photoluminescence quantum yield of THF solution (10^{-5} M in THF); PLQY^{film} – photoluminescence quantum yield of film; τ_1/τ_2 – fluorescence lifetimes;

For the better comparison purposes, four target compounds were divided into four pairs according to the structural similarities: compounds with same acceptor part (Pair 1 and 2) and compounds with same donor part (Pair 3 and 4). If to compare only fluorine-containing molecules BS-9 and BS-10 (Pair 1), we can observe that fluorescence spectra of solutions (both

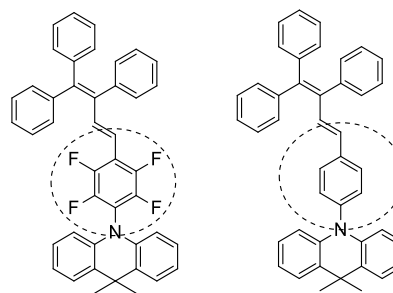
Pair 3:



BS-9

BS-12

Pair 4:



BS-10

BS-14

The presence of four electronegative Fluorine atoms highly increases the electron-accepting abilities of BS-9 and BS-10 in comparison with their non-fluorinated counterpart. In the case of Pair 3 fluorescence spectra of Toluene solution of non-fluorinated compound BS-12 is red-shifted if compare to the fluorinated one BS-9 with the peaks in Toluene at 434 nm (BS-9) and 448 nm (BS-12), when for Pair 4 it is vice versa with the fluorescence maxima peaks at 485 nm and 471 nm for BS-10 and BS-14 respectively. At the same time, presence of F atom reveals stronger ICT character for BS-9 than that of BS-12 (Pair 3). The same can be observed for BS-10 - solvatochromic properties of BS-10 are much stronger than that of non-fluorinated BS-14. Moderately higher PLQY values of solid films were examined for non-fluorinated compounds BS-12 and BS-14 in comparison to fluorinated BS-9 and BS-10 respectively.

The difference between the emission wavelength and the absorption wavelength (PL-ABS) is called as Stock's shift (Table 1). According to the calculated value we can say that the Stock's shift of the solution is higher than that of the film for sample BS-9 and vice versa for the sample BS-12.

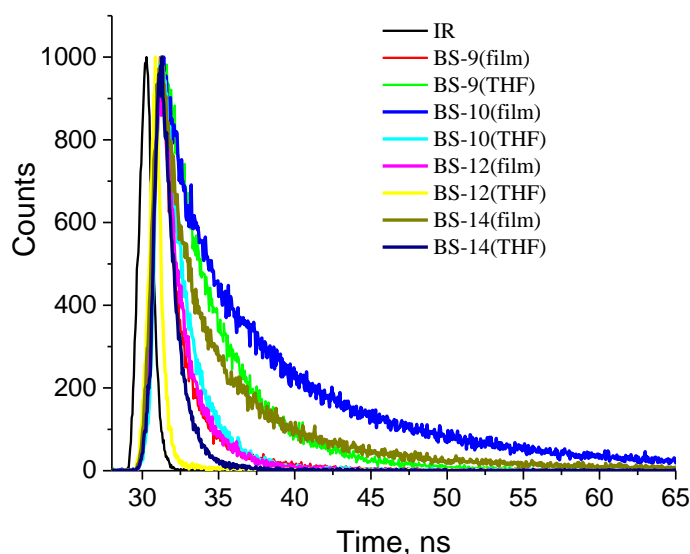


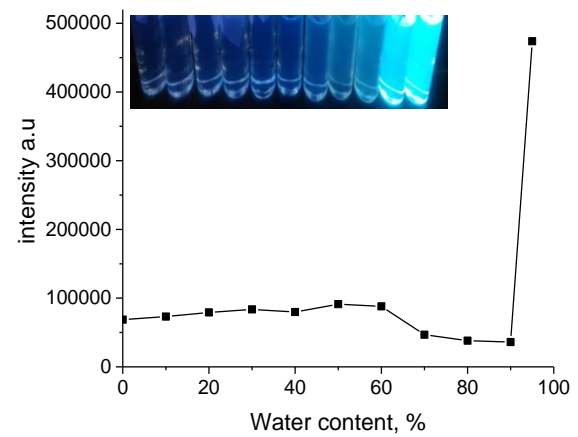
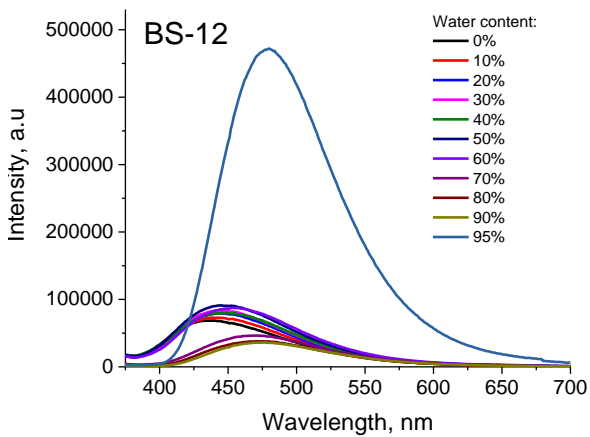
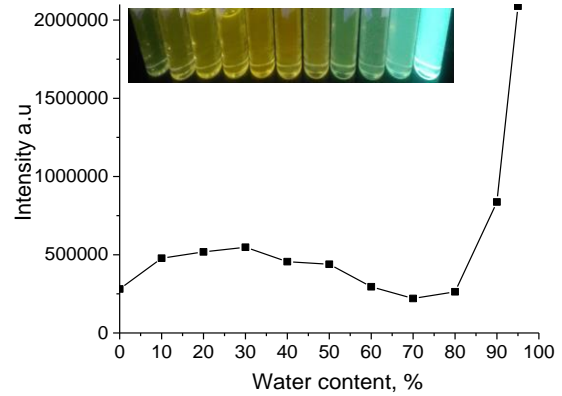
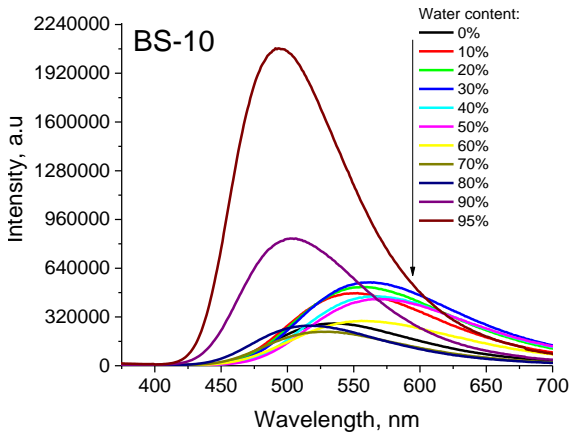
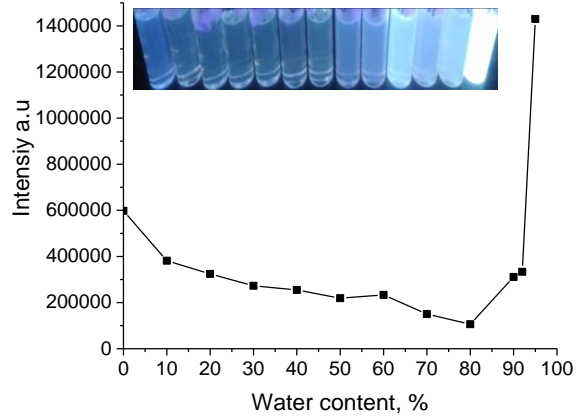
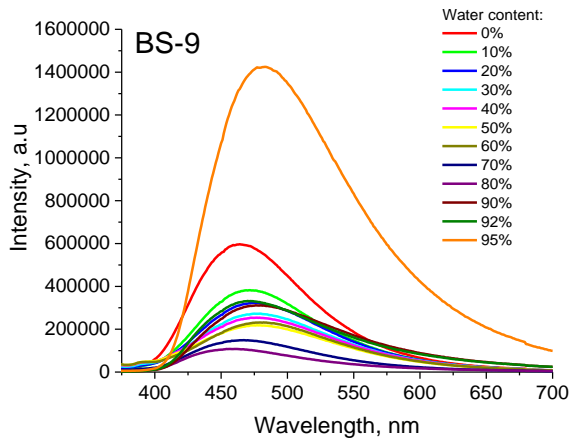
Fig. 15. Fluorescence decay curves of thin films and THF solutions

The fluorescence lifetimes of target compounds in dilute THF solutions and thin films were examined by recording fluorescence decay curves. The fluorescence decay curves of compounds 8 and 9 with the corresponding exponential fits are shown in Fig. 15 and the decay data parameters for all molecules is given in Table 2. The analysis of parameters shows that fluorescence decay of the compounds can be described by single or double exponential function. Two components are present in time decay of thin film of compounds. The longest fluorescence lifetime in THF solution was observed for fluorinated compounds BS-9 and BS-10 in comparison with non-fluorinated one.

4.2. Aggregation Induced Emission Enhancement

As it was mentioned before AIEE luminophores are possessing with low emission when molecularly dissolved in solvents due to active intramolecular rotations and vibrations but highly fluorescent in the crystalline state or during aggregation. It is known that triphenylethylene derivatives show AIE properties due to restricted intramolecular rotation (RIR) mechanism. To confirm AIEE properties of our four target molecules, fluorescence spectra of THF/water mixtures, with the different water content (starting from 0% and till 95% of water), were recorded and are shown in Fig. 16 (left). For the better evaluation of the properties, dependence of the amount of water in the sample and fluorescence intensity is also depicted at Fig. 16 (right). Carbazolyl-based molecule BS-12 shows weak emission in the pure

THF solvent, which is slightly decreasing with the addition of water till the water content, is reaching the value of 90% and then rise extensively, due to activation of RIR process.



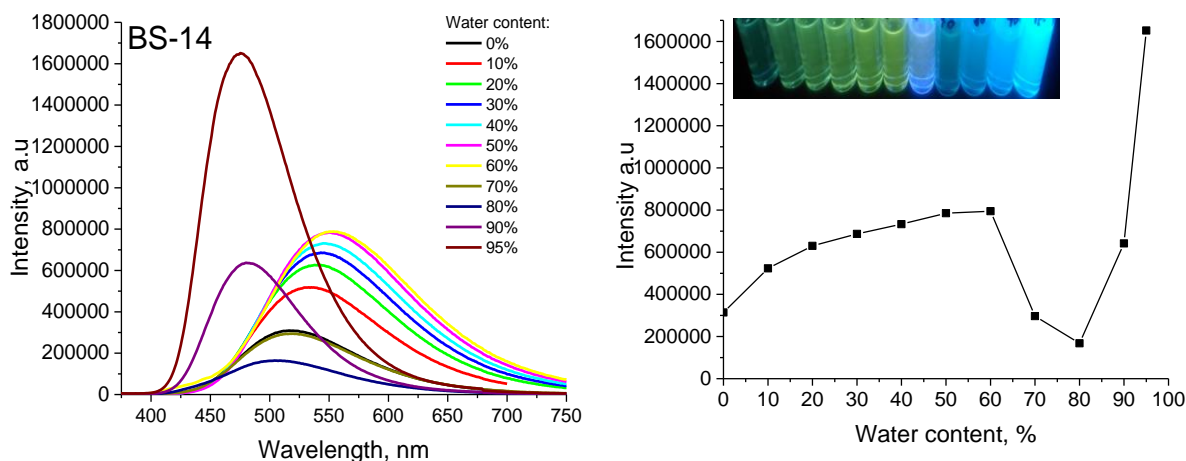


Fig. 16 (Left) Emission spectra of compounds in the THF/water mixtures with different water content. (Right) Plots of maximum emission intensities versus water content in the THF/Water mixtures. Solution concentration:

10 μ l. Excitation wavelength: 320 nm.

For its fluorinated congener BS-9 emission intensity firstly decrease till the 80% of water. At the point of 80% of water AIE mechanism activates for BS-9, resulting in emission enhancement in fourteen times for 95% of water in comparison with emission of the sample with 80% of water.

Interestingly, that for other two compounds, acridine-based BS-10 and BS-14, the emission intensity firstly increases till the water fraction reaching 30% for BS-10 and 60% for BS-14, then decrease till the value of 70% (BS-10) and 80% (BS-14) and then highly rise with the addition of water. Obviously, third enhancement of emission is due to the above mentioned RIR process (which activates AIEE). Increase and diminution of emission intensity during the addition of water before 70% for BS-10 and 80% for BS-14 can be explained by change of solvent polarity (water increase the solution polarity) and due to the presence of stronger donor (9,9-dimethylacridine in BS-10 and BS-14) and acceptor (Fluorine atoms in case of BS-10). As it is observed from the graph (Fig. 16) at a certain point (>70%) molecules begin to aggregate into nanoparticles and thus emit extensively, confirming the AIEE nature of our target compounds.

4.3. Photoelectrical and charge-transporting properties

An important characteristic of bipolar active compounds for the further fabrication and application in optoelectronic devices are ionization potential (I_p), which characterizes the electron releasing work under illumination. The hole-transporting and photoelectrical characteristics of compounds are presented in Table.3. Ionization potentials (I_p) were estimated from electron photoemission spectra of the amorphous films of the synthesized materials and are presented at Fig. 17. I_p values of solid samples estimated from photoemission spectra for synthesized compounds are in the range from 5.88 eV to 6.37 eV.

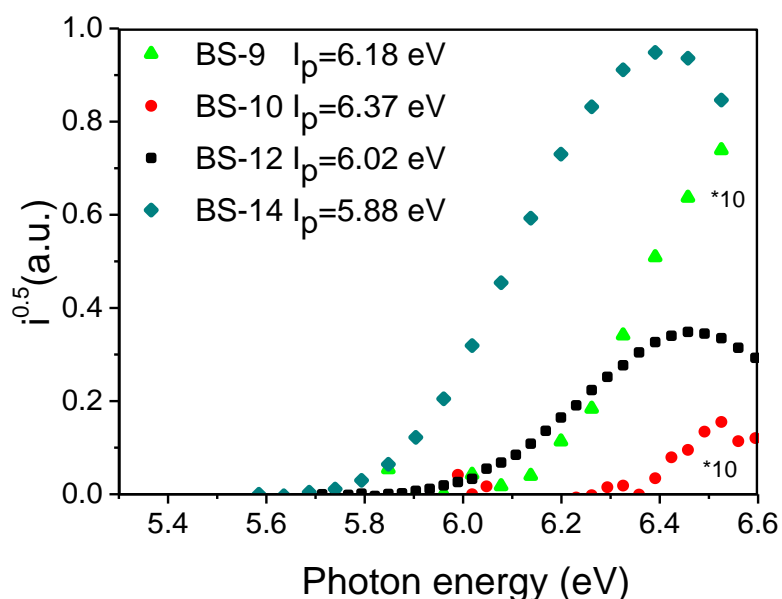


Fig. 17. Electron photoemission spectra of the films of four synthesized luminogens.

Compound	I_p , eV	EA, eV	E_g^{opt} , eV	μ_0 , $\text{cm}^{-1} \text{Vs}^{-2}$
BS-9	6.18	2.73	3.44	4.84×10^{-7} (at $5.67 \times 10^5 \text{ V/cm}$)
BS-10	6.37	2.89	3.48	5.80×10^{-4}
BS-12	6.02	2.71	3.31	3.07×10^{-3}
BS-14	5.88	2.30	3.58	1.97×10^{-3}

Table 3. Mobility spectra of compounds

I_p – ionization potential, estimated from photoemission spectra;

EA - electron affinity, estimated from the equation: $EA = I_p - E_g^{opt}$;

E_g^{opt} – optical band gap, estimated from the equation: $E_g^{opt} = 1240 / \lambda_{abs(peak)}^{film}$;

μ_0 - TOF hole-mobilities at $3.67 \times 10^5 \text{ V/cm}$ measured on vacuum evaporated films of compounds BS-9, BS-10, BS-12, BS-14;

Charge-transporting properties of the target compounds were investigated by the time of flight (TOF) technique. The TOF transients for holes and electrons of a thin layer of compounds are collected in Fig.18.

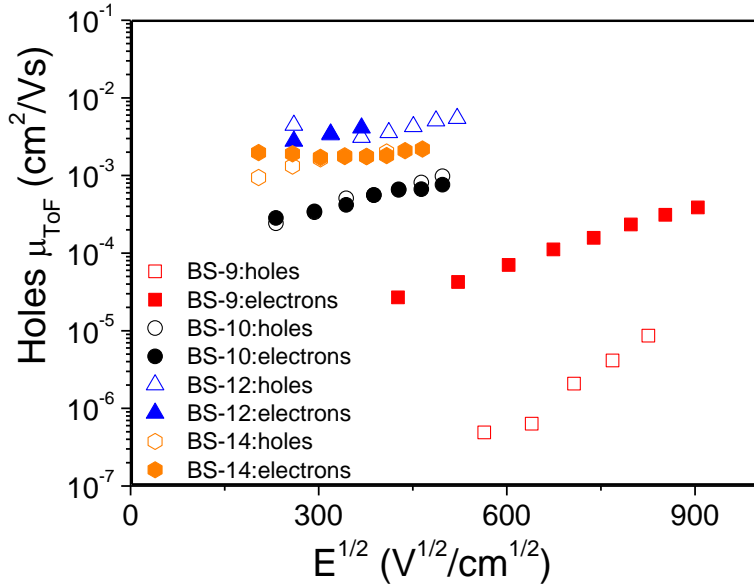
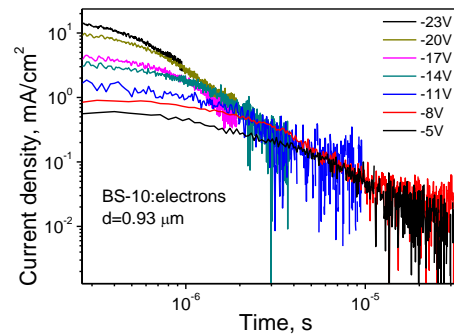
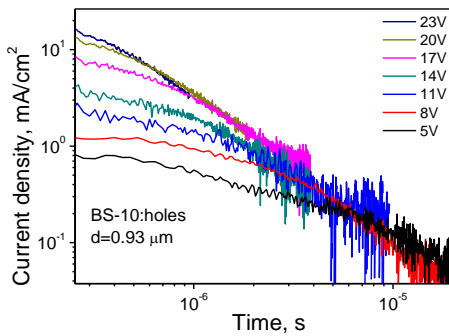
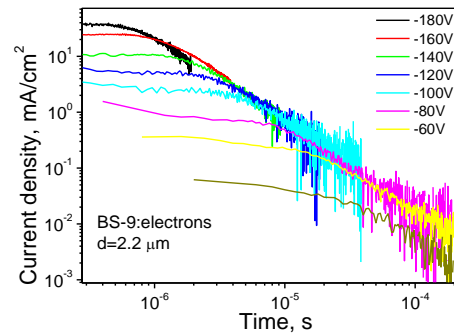
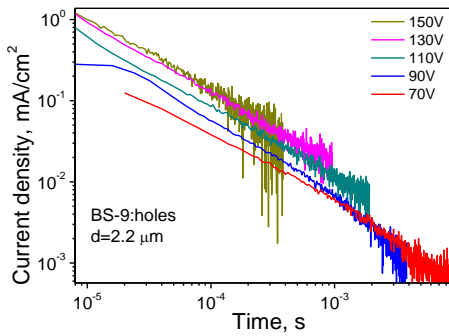


Fig. 18 Hole and electrons drift mobility as a function of $E^{1/2}$ for the layers of BS-9, BS-10, BS-12, BS-14.



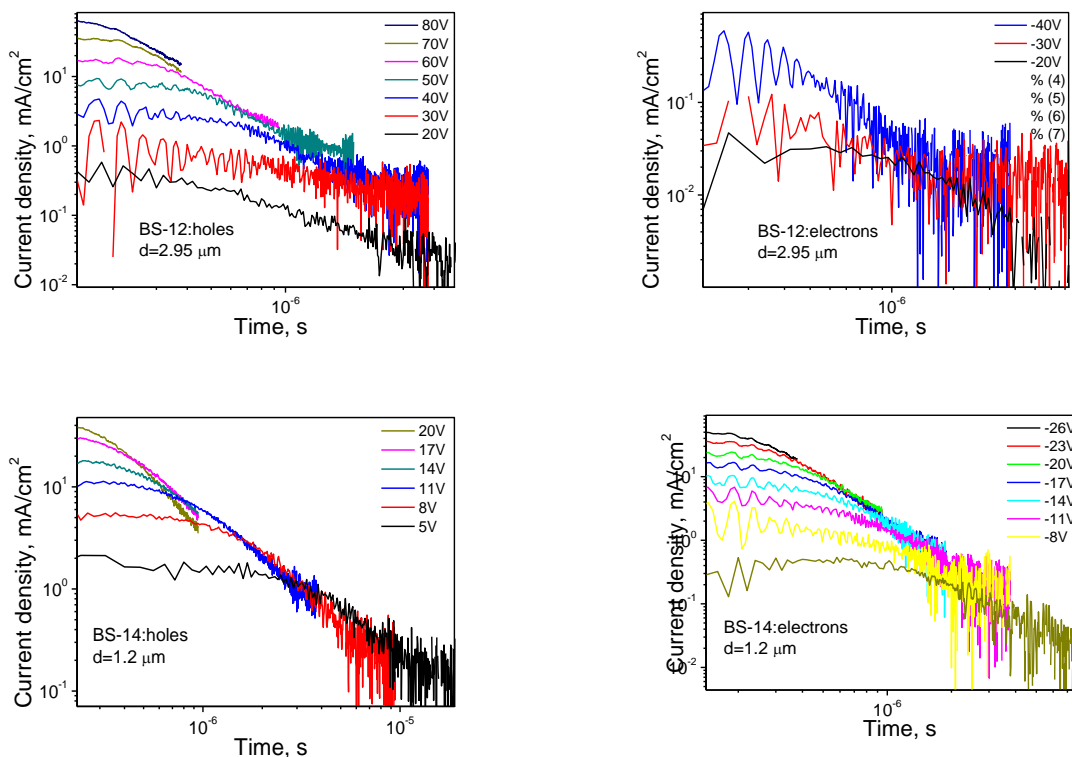


Fig. 19. Time of flight transients for holes in thin layers of compounds.

Balance between hole and electron charge transporting was observed for all molecules, except BS-9, which is characterized with higher electron mobility and lower hole drift mobilities (Fig. 19). Balanced and the highest hole and electron drift mobilities were found to be $3.07 \times 10^{-3} \text{ cm}^2/\text{Vs}$ (holes) and $4.2 \times 10^{-3} \text{ cm}^2/\text{Vs}$ (electrons) electric field of $3.67 \times 10^5 \text{ V/cm}$ for BS-12.

4.4. Thermal properties

Thermal properties of target compounds were studied by DSC and TGA under a nitrogen atmosphere. The values of glass transition temperatures (T_g), melting points (T_m) as well as temperatures of 5% weight loss (T_d) are summarized in Table.4. All four compounds are possessing with thig thermal stability with temperatures of 5% weight loss in the range from 307°C to 355°C as confirmed by TGA analysis with a heating rate of 10° C/min . Non-fluorinated compounds BS-12 and BS-14 are demonstrating higher values of T_d in comparison to their fluorinated analogues, with the highest T_d value of 355°C for BS-12. Moreover, the highest glass transition temperature of 123°C was observed also for compound BS-12. The DSC thermograms of all compounds are shown in Fig.20. TGA curves are depicted at Fig.20. Nonetheless, melting temperature for AIEgens are varying from 197°C to 263°C with the highest melting temperature for BS-14.

Compound	T _d , °C	T _g , °C	T _m , °C	T _c , °C
BS-9	343	116	197	-
BS-10	307	89	242	-
BS-12	355	123	244	-
BS-14	326	101	263	209

Table 4. Thermal properties of compounds: T_d - 5% weight loss temperature; T_g - glass formation temperature; T_m - melting point; T_{cr} – crystallization temperature;

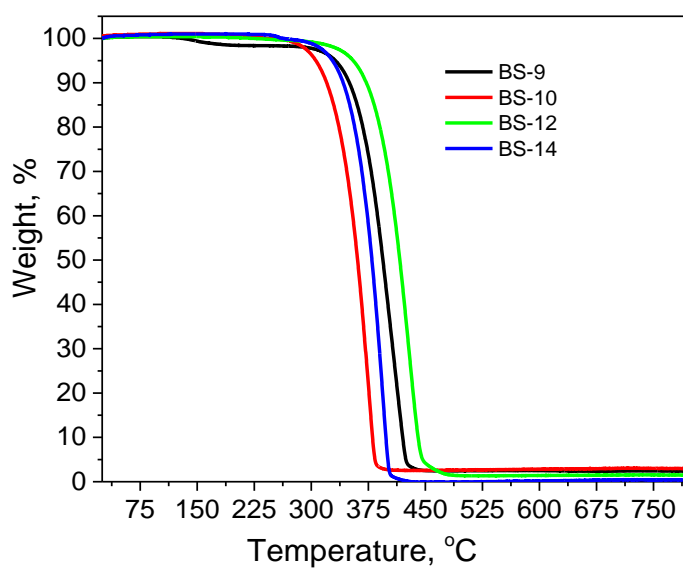


Fig. 20 TGA curves of compounds;

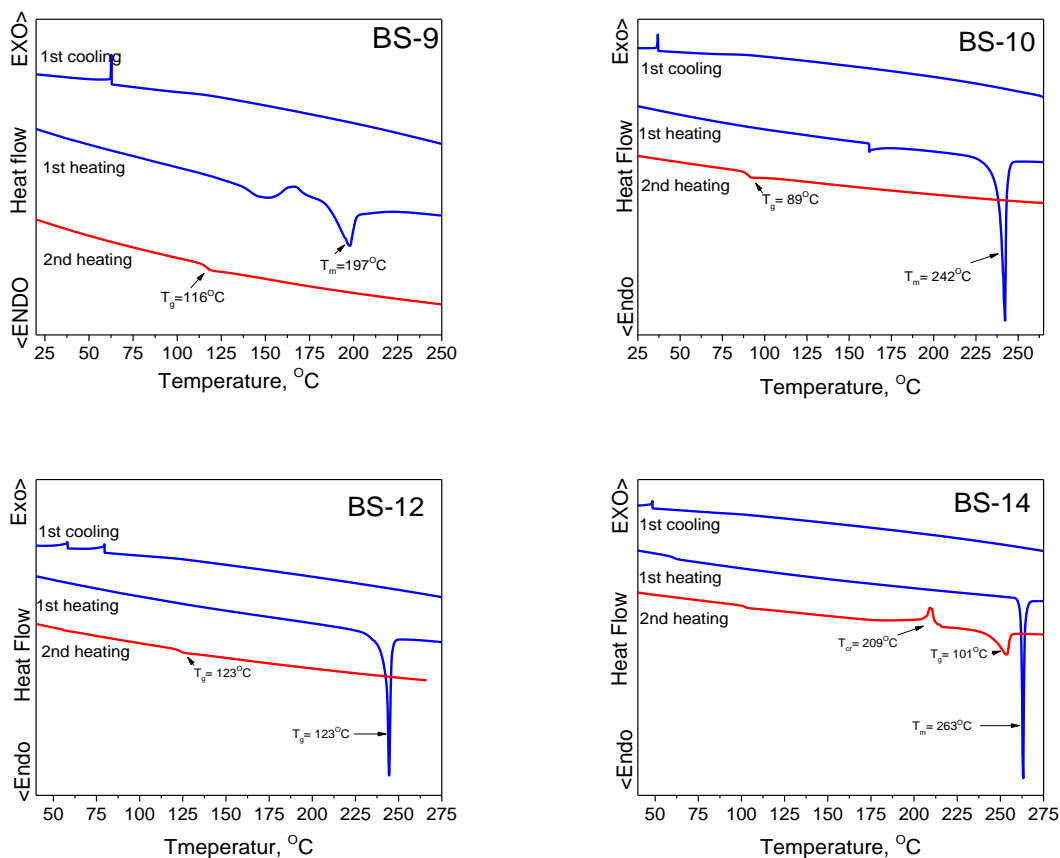


Fig. 21 DSC curves of BS-9, BS-10, BS-12 and BS-14;

During the synthesis all the materials were obtained as crystalline materials, nevertheless, they formed glasses during the second heating of the samples. However, during the DSC analysis crystallization process was observed only for BS-14 revealing crystallization temperature T_{cr} of 209 °C.

4.5. Device fabrication and characterization

Synthesized fluorescent emitters BS-10, BS-12 and BS-14 show high mobilities for both holes and electrons. Therefore, non-doped BS-10, BS-12 and BS-14 OLEDs with BS-10, BS-12 and BS-14 as emitting species respectively were fabricated to investigate its electroluminescent properties. Structures, energy levels and thickness of layers of the OLEDs are presented in Figure 1. Approximate HOMO energy levels of BS derivatives were taken from the ionization potential measurement. Estimation of the values of LUMO levels was done by subtracting optical band gaps from HOMO energy values. Electron affinity values (LUMO energies) were estimated from the equation: $EA = I_p - E_g^{opt}$, where E_g^{opt} is the optical band gap counted by the equation: $E_g^{opt} = 1240 / \lambda_{abs(peak)}^{film}$ ($\lambda_{abs(peak)}^{film}$ is the maxima of the last absorption peak).

Molybdenum trioxide was used as hole injection layer. Two hole transport layers of N,N'-di(1-naphthyl)-N,N'-diphenyl-(1,1'-biphenyl)-4,4'diamine (NPB) and 2,2',2''-tris-(N-carbazolyl)-triphenylamine (TCTA) were employed for bringing holes from the anode to the recombination site efficiently. HOMO levels of hole transport layers are alignment with each other in a way that stimulates transport of holes by overcoming smaller difference of energy levels more easily. Layer of TCTA can also operate as electron blocking layer [29]. Smaller thickness than of NPB layer and significant LUMO level differences with the emitting layers, especially for BS-10 and BS-12 (Figure 1), contribute to blocking of the electrons by TCTA. 2,2',2''-(1,3,5-benzinetriyl)-tris(1-phenyl-1-H-benzimidazole) (TPBi) was selected for the fabrication of electron transporting layer and lithium fluoride was employed as electron injection layer. Major electroluminescent characteristics of the devices made are presented in Table 5. The EL spectra at 8V are presented in Figure 23. In Figure 24 you can see the current density-voltage and luminance curves of the devices. The graphs of current, power and external quantum efficiencies are shown in Figures 25-27.

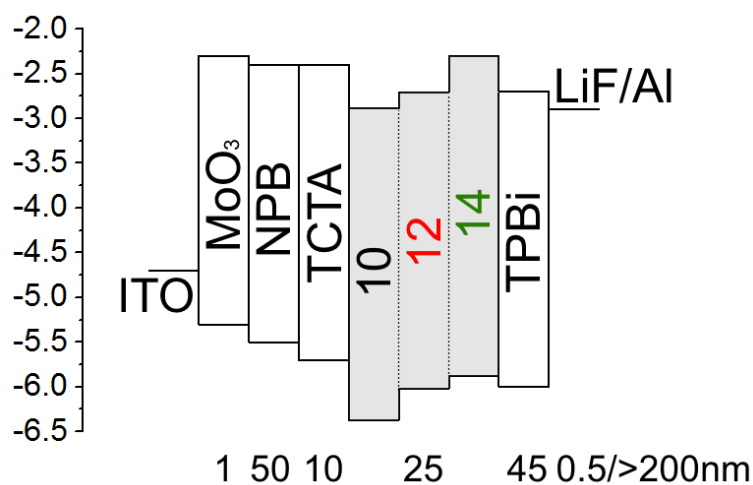


Fig. 22. Energy diagram of OLEDs

Device	Turn-on voltage, V	λ_{EL} peak, nm	Maximum brightness, 10^3cd/m^2	EQE maximum, %	Power efficiency maximum, lm/W	At 100cd/m^2 ^A	CIE coordinates ^B
BS-10	4.2	489	5.7	2	3.2	1.7%, 2.8 lm/W , 4.6 cd/A	0.20 0.35
BS-12	4.8	475	4.1	1.2	1.2	1.1%, 1.2 lm/W , 2.1 cd/a	0.17 0.25
BS-14	3.3	472	4.9	2	3.1	2%, 3 lm/W , 3.3 cd/A	0.16 0.21

Table 5. Electroluminescence parameters of OLEDs.

^AEQE, power and current efficiencies of devices at 100cd/m^2 . ^B CIE 1931 UCS coordinates at 8V [30].

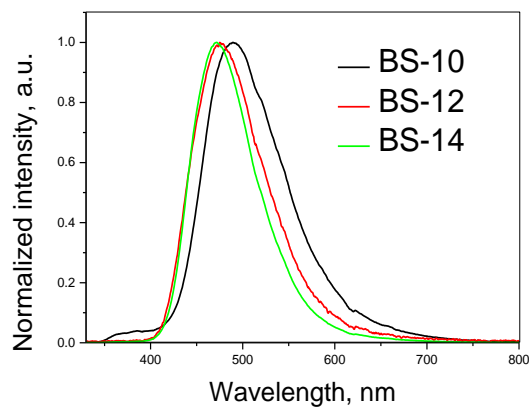


Fig. 23. Normalized electroluminescence spectra of OLEDs recorded at 8V.

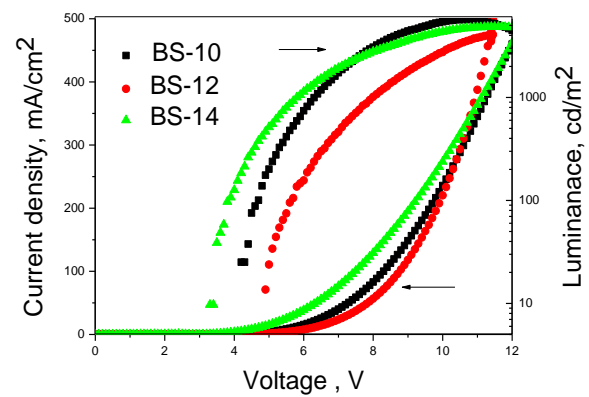


Fig. 24. Luminance and current density of OLEDs.

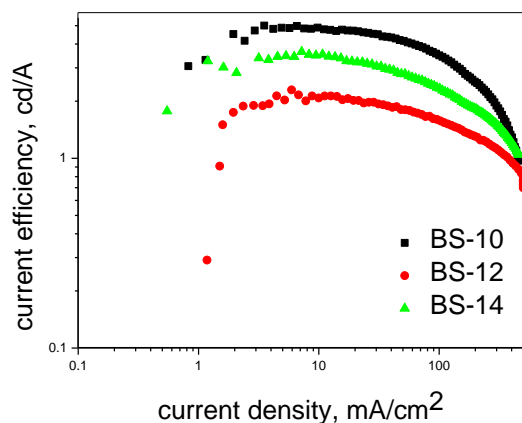


Fig. 25. Current efficiency of OLEDs.

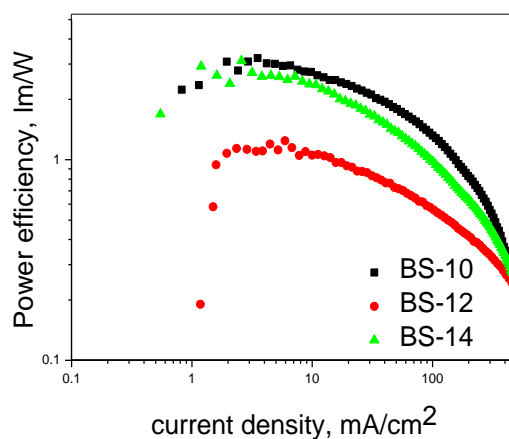


Fig. 26. Power efficiency of OLEDs.

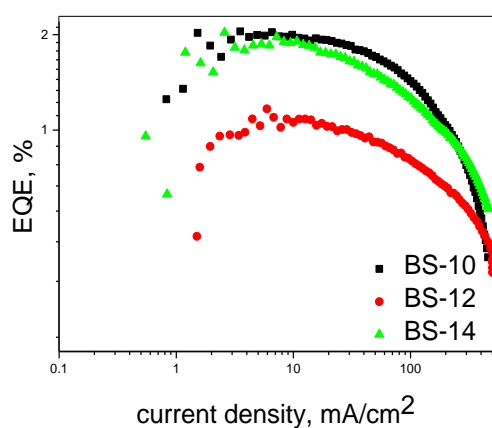


Fig. 27. EQE of OLEDs.

BS-10, BS-12 and 14 OLEDs performed sky-blue emission with the single emission peak at 489, 475 and 472nm, respectively. EL spectra are featureless (Figures 23, S1-4). It is a straightforward evidence of the absence of an exciplex/electroplex formation. Device's EL spectra representing well PL spectra of the neat film of derivative demonstrates clear radiative recombination attributed to investigated compounds.

The appropriate device structure can be also concluded not only from EL spectra analysis but from low turn-on voltages indicating good injection and transfer of holes and electrons from electrodes to an emitting layer. BS-14 has charge carriers mobilities bigger than BS-10. As the result, BS-14 has smaller turn-on voltage than BS-10, 3.3V versus 4.2V. 12 with the value of 4.8V and good charge transfer properties of BS12 contradict with such trend. Although corresponding of energy levels of transporting layers to emitting one seems to be better for BS-12 than for others, as it performed worse results on every characteristic out of all devices because of the lowest PLQY value. BS-10 and BS-14 both reached EQE of 2%, power

efficiency nearby 3.1 lm/W and maximum brightness of 5.5 and 4.9 thousand cd/m², respectively. Obtained values of EQE are in good agreement with the PLQY of compounds (Fig.28). 12 is less efficient than 10 or 14, almost in half. It is worth to mention that all devices showed typical roll-off dependence. At luminance of 100 cd/m² we can observe slightly lower than maximum values of efficiencies.

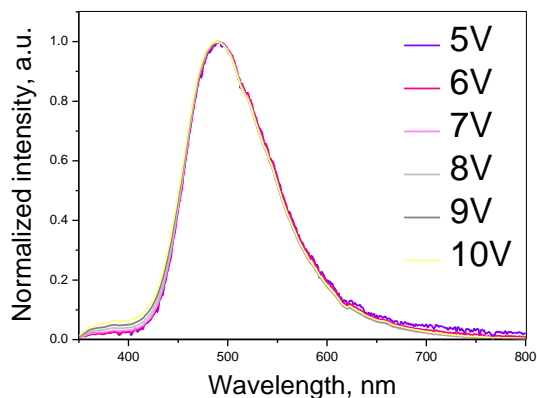


Fig. 28. EL spectra of 10 OLED.

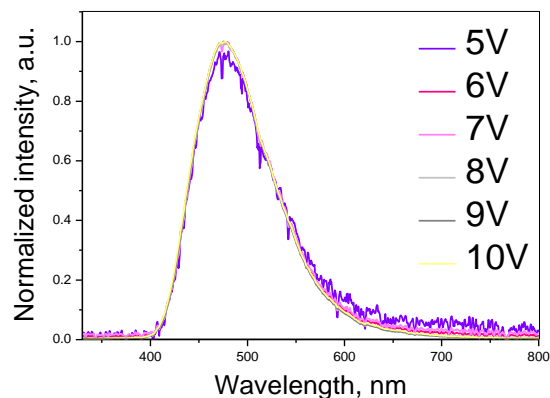


Fig. 29. EL spectra of 12 OLED.

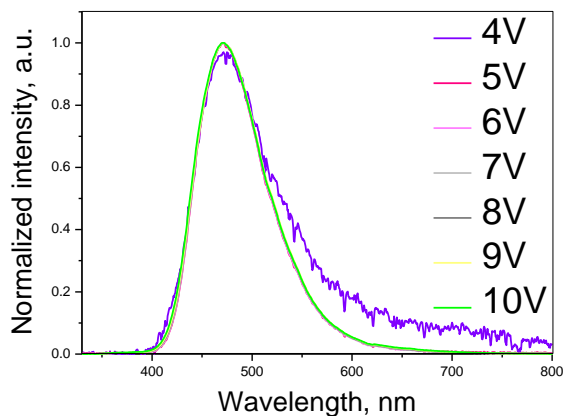


Fig. 30. EL spectra of 14 OLED.

5. Recommendations

In a tank the degassing of the solid compounds is performed. A1 used for starting material which is in the solid state into the tank, the a2 for ligand, a3 carries the base for the reaction mechanism, a5 is connected to the vacuum for the de-gas of the compounds, a4 is connected to an inert gas. The commonly used gasses are Nitrogen and Argon. The main purpose of this chamber is to make the compounds inert and the removal of oxygen between the molecules. This is done to prevent any unwanted interactions between the reactants and the surrounding environment.

In b-reaction chamber the solid compounds are transfer. The b1 carries the solvent for the reaction, b2 carries the starting material in liquid state, and b3 is used to supply inert gas for the neutral environment.

In c-extraction tank, the separation of the organic phase and the H₂O is performed, c1 is used to carry Dist-H₂O and c2 is used to carry the organic solvents, and c3 is used for the supply of air. These organic solvents have either higher or lower density compared to Dist-H₂O. Here the reaction mixture is mixed and when the air is supplied the organic phase is separated from the mixture. This organic phase is collected and transferred to the filtration tank.

In d-filtration tank the drying and filtering of the organic phase is performed. The organic phase is mixed with Na₂SO₄ and dried. It has a filter in middle of chamber for the separation of Na₂SO₄. The dried mixture is passed through a filter layer in the midpoint of the tank and collected at bottom. This separates the liquid filtrate form the solid Na₂SO₄. And the filtrate is transferred to the column.

Column-e is used for the separation of the sample form the impurities present in the filtrate. The e1 carries the silica gel, e2 is used for carrier eluent with measured ratio. Here the pure sample is separated and collected from the outlet at the bottom of the tank.

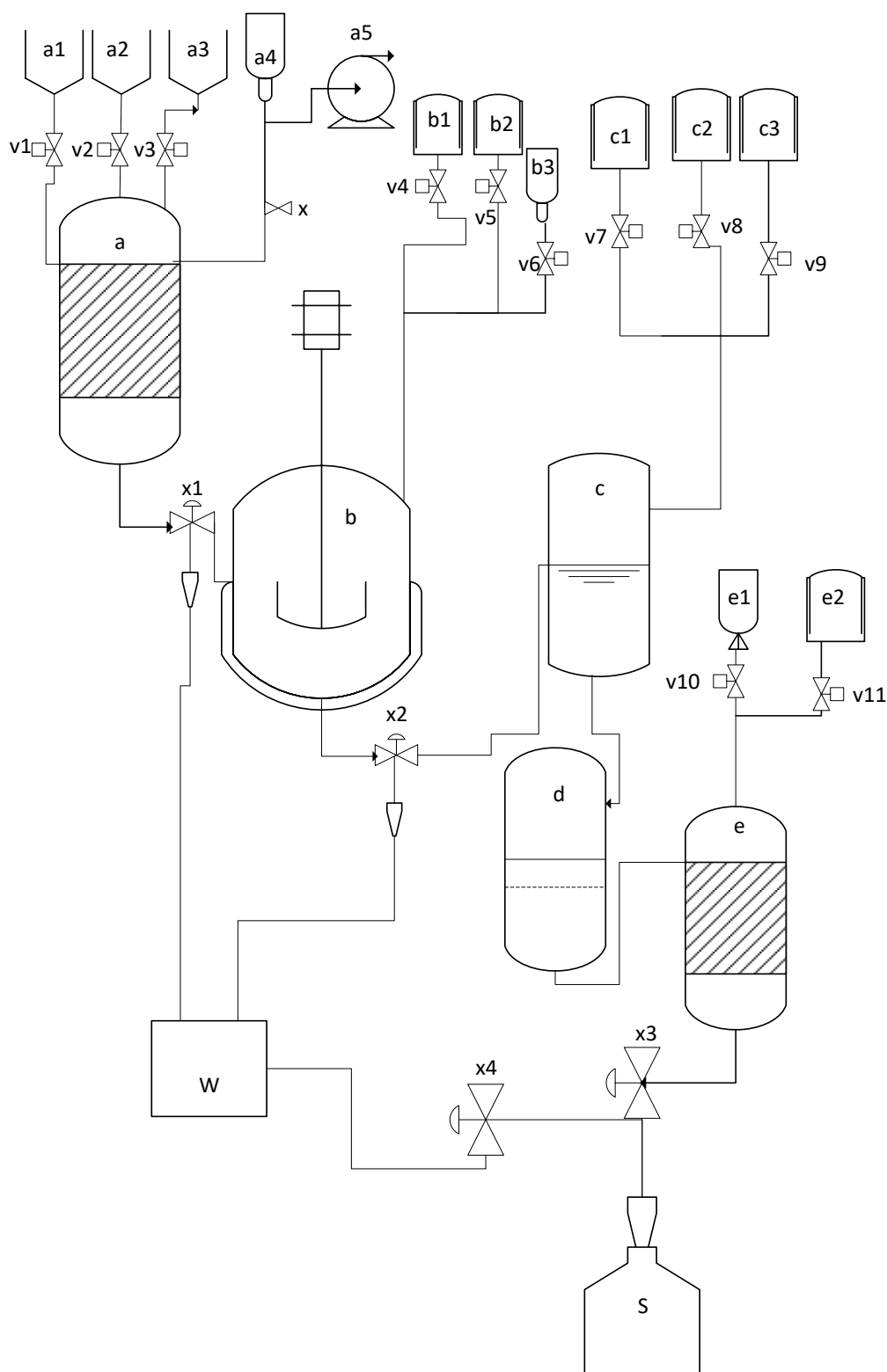


Fig 31. Schematics for reactor design: a – degassing tank, a1- starting material (solid), a2- ligand dispenser, a3-base dispenser, a4-inert gas cylinder (Argon/Nitrogen), a5-centrifugal pump (low pressure for vacuum), b - reaction tank, b1-starting material (liquid), b2-solvent for

reaction, b3- inert gas cylinder (Argon/Nitrogen), c-extraction tank, c1-organic solvent, c2-distilled water, c3-air, d-drying/filtration tank (with sodium sulphate on the top & filter in middle), e-column, e1-silica gel dispenser, e2-eluent, X-valve for argon/vacuum, x1-valve between a and b for transfer, x2- valve between b and c for transfer, x3- valve between e and s for collection, x4- valve between e and w for waster, V-sequence v1-v11 valves for controlling the flow system, W-waste, S-sample collection.

S-Sample collection tank. In this the sample is collected from the column and rotated to separate the liquid from the solid, to this solid sample an organic solvent is added to this tank. The solvent should have some specific properties. They are the sample should not be dissolved in this solvent when it is at room temperature or lower temperature, and when the temperature is increased the sample should dissolve in the solvent. This is called crystallization. It is used to wash the small impurities in the solid sample.

V-valves, the valves are connected to each chamber or tank containing different compounds or raw materials. Valves are used to control the flow of the materials and also to seal the vessels air tight for degassing of column usage

W- Waste tank is used to collect the organic/inorganic waste from the processing unit with the help of the outlets with valves. This waste is disposed in a designated disposable unit.

6. Employee's Safety and Health

6.1. Characteristics of designed materials

- a. Location of company: Faculty of Chemical Technology, 5th floor, Santaka Valley, K. Baršausko g. 59, Kaunas 51423, Lithuania.
- b. Purpose of company: To create an integrated science, study and business centre for public and private research, knowledge-intensive businesses, and to provide added-value services.
- c. Materials used: Carbazole, Zinc chloride, Tert-Butyl chloride, Tert-Butyl carbazole, Acridine, Nitro methane, Sodium sulfate, Silica Gel, Ethyl Acetate, Acetone, Iso-Propanol, 3,6-di-tert-butyl-9-(2,3,5,6-tetrafluoro-4-vinlyphenyl)-9Hcarbazole, Bromo triphenylethylene, Palladium (II) acetate, Triethyl Amine, Dimethyl Formamide, Tri(O-tolyl)phosphene, 10-(2,3,5,6-tetrafluoro-4-vinlyphenyl)-9,10-dihydro-9,9-dimethylacridine, Copper, Potassium carbonate, Tri-tert-butyl phosphene, Potassium tert-butoxide, Toluene, 3,6-di-tert-butyl-9-(4-vinlyphenyl)-9Hcarbazole, 9,10-dihydro-9,9-dimethyl-10-(4-vinlyphenyl) acridine, 4-Bromostyrene, Chloroform-d, Argon, Nitrogen.
- d. Synthesise products: BS-9: 3,6-di-tert-butyl-9-(2,3,5,6-tetrafluoro-4-((E)-3,4,4-triphenylbuta-1,3dienyl) phenyl)-9Hcarbazole, BS-10: 10-(2,3,5,6-tetrafluoro-4-((E)-3,4,4-triphenylbuta-1,3-dienyl) phenyl)-9,10-dihydro-9,9-dimethylacridine, BS-12: 3,6-di-tert-butyl-9-(4-((E)-3,4,4-triphenylbuta-1,3-dienyl) phenyl)-9Hcarbazole, BS-14: 9,10-dihydro-9,9-dimethyl-10-(4-((E)-3,4,4-triphenylbuta-1,3-dienyl) phenyl) acridine.

6.2. Occupational Risk Assessment

- a. Chemical agents

Compounds

Carbazole

Hazard symbol



Hazard statement

Specific Target Organ Toxicity –
Single exposure, categories 1,2
Specific Target Organ Toxicity –
Repeated exposure, categories
1,2
Aspiration Hazard, category 1

Zinc chloride



Corrosive to metals, category 1
Skin corrosion, categories 1A,1B,1C

Serious eye damage, category 1



Acute toxicity (oral, dermal, inhalation), category 4

Skin irritation, category 2

Eye irritation, category 2

Skin sensitisation, category 1

Specific Target Organ Toxicity – Single exposure, category 3

Hazardous to the aquatic environment

- Acute hazard, category 1

- Chronic hazard, categories 1,2



Silica Gel

Personal
Equipment

Protective Eye shields, Gloves, type N95 (US), type P1 (EN143) respirator filter.

RIDADR
WGK Germany

NONH for all modes of transport
Nwg.

Sodium sulfate

RIDADR
WGK Germany

NONH for all modes of transport
1

Tri(O-tolyl) phosphene

Personal
Equipment

Protective Dust mask type N95 (US), Eye shields, Gloves.

RIDADR
WGK Germany

NONH for all modes of transport.
3.

Tert-Butyl chloride,
Tert-Butyl carbazole,

Flammable gases, category 1
Flammable aerosols, categories

Acridine



Potassium carbonate,
4-Bromostyrene



Argon, Nitrogen



1,2

Flammable liquids, categories 1,2,3

Flammable solids, categories 1,2

Acute toxicity (oral, dermal, inhalation), category 4

Skin irritation, category 2

Eye irritation, category 2

Skin sensitisation, category 1

Specific Target Organ Toxicity – Single exposure, category 3

Acute toxicity (oral, dermal, inhalation), category 4

Skin irritation, category 2

Eye irritation, category 2

Skin sensitisation, category 1

Specific Target Organ Toxicity – Single exposure, category 3

Acute toxicity (oral, dermal, inhalation), category 4

Skin irritation, category 2

Eye irritation, category 2

Skin sensitisation, category 1

Specific Target Organ Toxicity – Single exposure, category 3

Gases under pressure:

- Compressed gases

- Liquefied gases

- Refrigerated liquefied gases

- Dissolved gases

Nitro methane



Flammable gases, category 1
Flammable aerosols, categories 1,2
Flammable liquids, categories 1,2,3
Flammable solids, categories 1,2
Acute toxicity (oral, dermal, inhalation), categories 1,2,3
Respiratory sensitization, category 1



Germ cell mutagenicity, categories 1A,1B,2
Carcinogenicity, categories 1A,1B,2
Reproductive toxicity, categories 1A,1B,2



Specific Target Organ Toxicity – Single exposure, categories 1,2
Specific Target Organ Toxicity – Repeated exposure, categories 1,2
Aspiration Hazard, category 1

Ethyl Acetate,
Acetone,
Iso-Propanol



Flammable gases, category 1
Flammable aerosols, categories 1,2
Flammable liquids, categories 1,2,3
Flammable solids, categories 1,2
Acute toxicity (oral, dermal, inhalation), categories 1,2,3
Respiratory sensitization, category 1

Triethyl Amine



Acute toxicity (oral, dermal, inhalation), category 4
Skin irritation, category 2
Eye irritation, category 2
Skin sensitisation, category 1
Specific Target Organ Toxicity – Single exposure, category 3

Flammable gases, category 1
Flammable aerosols, categories 1,2

Flammable liquids, categories 1,2,3

Flammable solids, categories 1,2

Acute toxicity (oral, dermal, inhalation), categories 1,2,3

Respiratory sensitization, category 1

Corrosive to metals, category 1

Skin corrosion, categories 1A,1B,1C

Serious eye damage, category 1

Germ cell mutagenicity, categories 1A,1B,2

Carcinogenicity, categories 1A,1B,2

Reproductive toxicity, categories 1A,1B,2

Flammable gases, category 1

Flammable aerosols, categories 1,2

Flammable liquids, categories 1,2,3

Flammable solids, categories 1,2

Dimethyl Formamide,
Toluene



Copper



Acute toxicity (oral, dermal, inhalation), categories 1,2,3

Respiratory sensitization, category 1

Acute toxicity (oral, dermal, inhalation), category 4

Skin irritation, category 2

Eye irritation, category 2

Skin sensitisation, category 1

Specific Target Organ Toxicity – Single exposure, category 3

Specific Target Organ Toxicity – Single exposure, categories 1,2

Specific Target Organ Toxicity – Repeated exposure, categories 1,2

Aspiration Hazard, category 1

Hazardous to the aquatic environment

- Acute hazard, category 1

- Chronic hazard, categories 1,2

Flammable gases, category 1

Flammable aerosols, categories 1,2

Flammable liquids, categories 1,2,3

Flammable solids, categories 1,2

Acute toxicity (oral, dermal, inhalation), categories 1,2,3

Respiratory sensitization, category 1

Tri-tert-butyl phosphene,
Potassium tert-butoxide



Flammable gases, category 1
Flammable aerosols, categories 1,2
Flammable liquids, categories 1,2,3
Flammable solids, categories 1,2
Acute toxicity (oral, dermal, inhalation), categories 1,2,3
Respiratory sensitization, category 1
Corrosive to metals, category 1
Skin corrosion, categories 1A,1B,1C
Serious eye damage, category 1



Chloroform-d



Germ cell mutagenicity, categories 1A,1B,2
Carcinogenicity, categories 1A,1B,2
Reproductive toxicity, categories 1A,1B,2
Specific Target Organ Toxicity – Single exposure, categories 1,2
Specific Target Organ Toxicity – Repeated exposure, categories 1,2
Aspiration Hazard, category 1



Description of materials and its hazardous properties [31]

b. Physical factors

Factors	Values standards	Lithuania standards
Thermal environment	Summer: 22.8 °C to 26.1 °C Winter: 20.0 °C to 23.9 °C [32]	HN 69: 2003
Noise	$L_{EX,8h} = 85$ dBA, $L_{Cpeak} = 137$ Dbc;	HN 33: 2011
Air pollution	(8 OU_E / m^3). [33]	HN 23: 2011
Illumination	1000 lumens/ m^2	HN 98: 2014
Equipment grounding	TT-system TN-system IT-system	(Elektros įrenginių įrengimo taisyklės. Vilnius, 2000. 487 p. [34] Saugos taisyklės eksploatojant elektros įrenginius, Valstybės žinios, 2001, nr. 110-4008) [35]

Table. 6 physical factors standards and lab readings

L_{EX} - Lower exposure action

L_{Cpeak} - C-weighted sound pressure level,

TT-system- One point at the supply source is connected directly to earth. All exposed and extraneous conductive parts are connected to a separate earth electrode at the installation. Earth electrode must have a low resistance to be able trip the circuit breaker. But sometimes it is difficult to achieve low resistance. Therefore, RCD device must be used to protect for leakage current in the circuit. PE and N must never be connected.

c. Trauma related physical factors

Equipment	Injuries
Heating plate	Hand burns
Glass ware	Cuts in hands and legs

d. Ergonomic factors

Standing and working in awkward positions in laboratory hoods.

e. Psychological factors

Long working hours and uncomfortable working environment causes the psychological stress.

6.3. Safe production

To ensure protection against exposure to electric current:

- All metal parts of electric equipment must be nullified or earthed.
- Voltage-bearing parts must be protected against contact with them; electrical wiring insulation may not be damaged.
- Plugs and sockets must be in a good technical condition.

With the above safety regulations, the laboratory comes under the category of “General Premises” [36].

- Electrical equipment neutral connection

All the 400 V or higher AC and 440V or higher DC equipment are grounded for the safety and prevention of explosion in laboratory due to electrical failure or equipment’s damage.

- The maximum activation for the low voltage and daily usage equipment is 0.2 sec to 0.3 sec. this is a little higher than the standard 0.2 sec. To avoid any type of damage the inspection on equipment is conducted every 6 months and the delays or time lags are fixed in that inspection by the technicians.

6.4. Hygiene standards

Factors	Lithuania standards	Determine the working standard (analysed)
Thermal environment	HN 69: 2003	Summer: 20 °C to 25 °C Winter: 18 °C to 20 °C
Noise	HN 33: 2011	$L_{EX,8h} = 95$ dBA, $L_{Cpeak} = 130$ Dbc;
Air pollution	HN 23: 2011	According to the standards in previous tale
Illumination	HN 98: 2014	150-205 lumens/ m ²
Equipment grounding	(Elektros įrenginių įrengimo taisyklės. Vilnius, 2000. 487 p. [34] Saugos taisyklės eksploatojant elektros įrenginius, Valstybės žinios, 2001, nr. 110-4008) [35]	TT-system

Table 7. Hygiene and determined working standards.

- Personal protective equipment

Safety-toe footwear, Prescription safety eyewear, Everyday clothing and weather-related gear, Logging boots.

- Safety Glasses

Much stronger and more resistant to impact and heat than regular glasses. Equipped with side shields that give you protection from hazards that may not be directly in front of you. Safety glasses should be Z-87 approved to meet OSHA regulations. Should fit comfortable on face through all job tasks. Ensure that glasses are not too big or too tight. Limitation: Does not seal around eyes, leakage of small droplets into eyes.

- **Face Shields**

Full face protection. It is used around operations which expose you to molten metal, chemical splashes, or flying particles. Can be used simultaneously as a hard hat. Limitations are not considered eye protection, will need to wear goggles or glasses underneath, can fog up if working in poorly ventilated area.

6.5. Fire Safety

- If laboratory worker's clothing catches fire, not to allow the victim to run around the laboratory but to immediately throw a woollen wrap, jacket or robe and pour water on him/her.
- In case of fire a student must:
 - Immediately report fire to a fire prevention service by a single emergency number '112' and the laboratory work supervisor.
 - Put out all burners, disconnect electrical equipment and operating apparatuses;
 - Inform people about the fire and extinguish the fire source using available devices.
 - Operating electrical equipment may be extinguished only with carbon dioxide extinguishers [36].

7. Conclusions

1. New derivatives carbazole and 9,9-dimethylacridine containing triphenylethylene moieties were designed, synthesized, and investigated;
2. It was shown by fluorescence measurements of water/THF mixtures that the synthesized compounds the phenomenon of aggregation induced emission enhancement.
3. The synthesized luminogens exhibit solvatochromism which is explained by intramolecular charge transfer;
4. Photoluminescence quantum yields of dilute solutions and solid films of the synthesized were estimated for both solutions and films of the compounds and were found to be in the range of 0.1-11% for solutions and of 16-29% for the films; this observation confirms the AIEE nature of the molecules.
5. All four compounds possess high thermal stability with 5% weight loss temperatures in the range from 307 °C to 355 °C. The synthesized molecules form glasses with glass transition temperatures ranging from 89 °C to 123 °C.
6. The solid-state ionization potentials and electron affinities were found to be in the ranges of 5.88-6.37 eV and 2.30-2.89 eV, respectively.
7. The compounds were implemented in OLEDs as emitters. The highest external quantum efficiency of 2% was observed for the devices based on emitters containing 9,9-dimethylacridine moieties.

8. Acknowledgments

Firstly, I would like to thank my supervisor prof. Juozas Vidas Grazulevicius, Head of Department of Polymer Chemistry and Technology. He gave me this wonderful opportunity to study and prepare my master's thesis in his research group, for all the support and encouragement that he gave for the successful completion of my thesis at Kaunas University of Technology.

My sincere thanks to my consultant Ph.D. student Galyna Sych, for teaching me techniques of the organic synthesis, for being patient while explaining the procedures and mechanisms of the reactions and analytical tools like UV-VIS, PL-spectra, lab related equipment and analysis software's like Chem Draw and MestRe Nova and for helping me in writing my thesis. Truly her guidance was very helpful throughout my thesis.

I also like to thank the remaining members of the group prof. Dr. Gintaras Buika, Rasa Keruckiene, Ramin Peahazadeh, Victoria Mimaite, Tomas Matulaitis, Greta Ragaite, Sohrab Nasiri, Oleksandr Bezikonnyi, Dmytro Volyniuk, Jurate Simokaitiene, Egle Jatautiene, Audrius Buciskas, Jonas Keruckas, Edgaras Narbutaitis. They made the lab very enjoyable, the fun in doing the research and for helping me in my master's research in different analysis, suggestions for the reaction mechanisms, product separation and software etc.

Finally, I would like to thank my international student co-ordinator Dr. Dovile Sinkeviciute for helping me in each issue in the rules, registration, and other academic related situations, and my department/academic co-ordinator for chemical engineering Dr. Irmantas Barauskas, who was a teacher for me in several subjects and helped in the understanding of rules and regulations of the academics.

9. References

1. Tang, C.W.; VanSlyke, S.A. Organic electroluminescent diodes, *Appl. Phys. Lett.*, 1987, vol. 51, p. 913-915.
2. Luo, J.; Xie, Z.; Lam, J.W.Y.; Cheng, L.; Chen, H.; Qiu, C.; Kwok, H.S.; Zhan, X.; Liu, Y.; Zhuc, D.; Tang, B.Z. Aggregation-induced emission of 1-methyl-1,2,3,4,5-pentaphenylsilole, *Chem. Commun.*, 2001, vol. 18, p. 1740–1741.
3. Roldán-Carmona, C.; Malinkiewicz, O.; Soriano, A.; Espallargas, G.M.; Garcia, A.; Reinecke, P.; Kroyer, T.; Ibrahim, D.M.; Nazeeruddin, M.K.; Bolink, H.J. Flexible high efficiency perovskite solar cells, *Energy Environ. Sci.*, 2014, vol. 7, p. 994-997.
4. Leung, N.L.C.; Xie, N.; Yuan, W.; Liu, Y.; Wu, Q.; Peng, Q.; Miao, Q.; Lam, J.W.Y.; Tang, B.Z. The general mechanism behind aggregation-induced emission, *Chem. Eur. J.*, 2014, vol. 20, p. 1–6.
5. Foster, V.T.H.; Kasper, K. Ein konzentrationsumschlag der fluoreszenz des pyrens, *Z. Physik. Chem.*, 1954, vol. 275, p. 976-980.
6. Bhongale, C. J.; Chang, C.W.; Lee, C.S.; Diao, E. W.G.; Hsu, C.S. Relaxation dynamics and structural characterization of organic nanoparticles with enhanced emission, *J. Phys. Chem. B.*, 2005, vol. 109, p. 13472–13482.
7. Mei, J.; Hong, Y.; Lam, J.W.Y.; Qin, A.; Tang, Y.; Tang, B.Z. Aggregation-induced emission: The whole is more brilliant than the parts, *Adv. Mater.*, 2014, vol. 26, p. 5429–5479.
8. Ma, X.; Rui, S.; Cheng, J.; Liu, J.; Fei, G.; Xiang, H.; Zhou, X. Fluorescence aggregation-caused quenching versus aggregation induced emission, *J. Chem. Educ.*, 2016, vol. 93, p. 345–350.
9. (a) Chen, J.; Law, C.C.W.; Lam, J.W.Y.; Dong, Y.; Lo, S.M.F.; Williams, I.D.; Zhu, D.; Tang, B.Z. Synthesis, light emission, nano-aggregation, and restricted intramolecular rotation of 1,1-substituted 2,3,4,5-tetraphenylsiloles, *Chem. Mater.*, 2003, vol. 15, p. 1535–1546.
(b) Jin, J.K.; Sun, J.Z.; Dong, Y.Q.; Xu, H.P.; Yuan, W.Z.; Tang, B.Z. Aggregation-induced emission of an aminated silole: A fluorescence probe for monitoring layer-by-layer self-assembling processes of polyelectrolytes, *J. Lumin.*, 2009, vol. 129, p. 19–23.
10. Sakalyte, A.; Simokaitiene, J.; Tomkeviciene, A.; Keruckas, J.; Buika, G.; Grazulevicius, J.V.; Jankauskas, V.; Hsu, C.P.; Yang, C.H. Effect of methoxy

- substituents on the properties of the derivatives of carbazole and diphenylamine, *J. Phys. Chem. C*, 2011, vol. 115, p. 4856–4862.
11. Yang, Z.; Chi, Z.; Xu, B.; Li, H.; Zhang, X.; Li, X.; Liu, S.; Zhang, Y.; Xu, Ji. High-Tg carbazole derivatives as a new class of aggregation-induced emission enhancement materials, *J. Mater. Chem*, 2010, vol. 20, p. 7352-7359.
 12. Kwok, R.T.K.; Leung, C.W.T.; Lam, J.W.Y.; Tang, B.Z. Biosensing by luminogen with aggregation induced emission characteristics, *Chem. Soc. Rev*, 2015, vol. 44, p. 4228-4238.
 13. Lee, Y.T.; Chang, Y.T.; Chen, C.T.; Chen, C.T. The first aggregation-induced emission fluorophore as a solution processed host material in hybrid white organic light-emitting diodes, *J. Mater. Chem. C*, 2016, vol. 4, p. 7020-7025.
 14. Reghu, R.R.; Volyniuk, D.; Kostiv, N.; Norvaisa, K.; Grazulevicius, J.V. Symmetry versus asymmetry: Synthesis and studies of benzotriindole derived carbazoles displaying different electrochemical and optical properties, *Dyes Pigm*, 2016, vol. 125, p. 159-168.
 15. Shirota, Y; Kageyama, H. Small molecular weight materials for (opto)electronic applications, Woodhead Publishing Limited, 2013, 3 p.
 16. Scholl, A.; Schreiber, F. Thin films of organic molecules: interfaces and epitaxial growth, Elsevier Inc, 2013, 591 p.
 17. Patel, B. N.; Prajapati, M. M. OLED: A modern display technology, *IJSRP*, 2014, vol. 4, p. 2250-3153.
 18. Natali, D.; Caironi, M. Photodetectors: Materials, devices and applications, Elsevier Science & Technology, UK, 2015, vol. 1, p. 195–254.
 19. Dijken, A.V.; Bastiaansen, J.J.A.M.; Kikken, N.M.M.; Langeveld, B.M.W.; Rothe, C.; Monkman, A.; Bach, I.; Stossel, P.; Brunner, K. Carbazole compounds as host materials for triplet emitters in organic light-emitting diodes: Polymer hosts for high-efficiency light-emitting diodes, *J. Am. Chem. Soc*, 2004, vol. 126, p. 7718–7727.
 20. Tomkeviciene, A.; Grazulevicius, J.V. Glass-forming organic semiconductors for optoelectronics, *Mater. Sci.*, 2011, vol. 17, p. 335-342.
 21. Lee, H.N.; Kim, H.N.; Swamy, K.M.K.; Park, M.S.; Kim, J.; Lee, H.; Lee, K.H.; Park, S.; Yoon, J. New acridine derivatives bearing immobilized azacrown or azathiacrown ligand as fluorescent chemo-sensors for Hg²⁺ and Cd²⁺, *Tetrahedron Lett*, 2008, vol. 49, p. 1261–1265.

22. Wang, Y.; Hua, X.Y.; Wang, L.; Shanga, Z.B.; Chao, J.B.; Jin, W. A new acridine derivative as a highly selective 'off-on' fluorescence chemo-sensor for Cd²⁺ in aqueous media, *Sensors and Actuators B*, 2011, vol. 156, p. 126–131.
23. Reddy, S.S.; Gopalan, V.S.; Kumarasamy G.; Cho, W.; Gal, Y.S.; Song, M.; Kang, J.W.; Jin, S.H. Highly efficient bipolar deep-blue fluorescent emitters for solution-processed non-doped organic light-emitting diodes based on 9,9-Dimethyl-9,10-dihydroacridine/ Phenanthroimidazole derivatives. *Adv. Optical Mater*, 2016, vol. 4, p. 1-11.
24. Wang, Y.K.; Yuan, Z.C.; Shi, G.Z.; Li, Y.X.; Li, Q.; Hui, F.; Sun, B.Q.; Jiang Z.Q.; Liao, L.S. Dopant-free spiro-triphenylamine/fluorene as hole transporting material for perovskite solar cells with enhanced efficiency and stability, *Adv. Funct. Mater*, 2016, vol. 26, p. 1375–1381.
25. Wex, B.; Bilal Kaafarani, R. Perspective on carbazole-based organic compounds as emitters and hosts in TADF applications, *J. Mater. Chem. C*, 2017, vol. 5, 8622-8653 p.
26. Price, C. C. *Organic reactions*, John Wiley and Sons, Inc, Canada, 2011, 2 p.
27. Eyley, S. C. *The aliphatic friedel-crafts*. Elsevier, Oxford, UK, 1991, 707 p.
28. Gudeika, D.; Sini, G.; Jankauskas, V.; Sych, G.; Grazulevicius, J.V. Synthesis and properties of the derivatives of triphenylamine and 1,8-naphthalimide with the olefinic linkages between chromophores, *RSC Adv*, 2016, vol. 6, p. 2191-2201.
29. Hu, R.; Lager, E.; Angelica, A.A.; Liu, J.; Lam, J.W.Y.; Sung, H.H.Y.; Williams I.D.; Zhong, Y.; Wong, K.S.; Cabrera, E.P.; Tang, B.Z. Twisted intramolecular charge transfer and aggregation-Induced emission of bodipy derivatives, *J. Phys. Chem. C*, 2009, vol. 113, p. 15845–15853.
30. Yang, X.; Mutlugun, E.; Zhao, Y.; Gao, Y.; Leck, K. S.; Ma, Y.; Ke, L.; Tan, S. T.; Demir, H. V.; Sun, X. W. Solution processed tungsten oxide interfacial layer for efficient hole-injection in quantum dot light emitting diodes, *Small*, 2014, vol. 10, p. 247–252.
31. Smith, T.; Guild, J. The C.I.E. colorimetric standards and their use, *Trans. Opt. Soc.*, 1931, vol. 33, p.73-134.
32. Data sheet of compounds, symbols, and statements [online]. In Sigma-Aldrich, 2018 [viewed 22 05 2018]. Available from <https://www.sigmaaldrich.com/european-export.html>.
33. Kebblas, A.; Regulations and control – experience in Lithuania, *National Public Health Surveillance Laboratory*, 2015, 1 p.

34. Elektros linijos ir instaliacija, Vilnius-Lietuvos energetikų mokslo ir technikos draugijos ind. įm, 2000, 487 p.
35. Elektros įrenginių eksploatavimo saugos taisyklės, patvirtintos Lietuvos. Asmenų, kurie privalo įgyti žinių sveikatos klausimais, profesijų sąrašas, 2001, 52 p.
36. Prof. Valatka, E. Safety and health instructions for student carrying out laboratory and research work at the training and science laboratory of the unit of polymer chemistry and technology laboratories, Faculty of Chemical Technology, 2017, 1 p.